CHARLES UNIVERSITY
Faculty of Pharmacy in Hradec Králové
Department of Pharmacology and Toxicology

ALTERATIONS IN GENE EXPRESSION OF HEPATOBILIARY TRANSPORTERS AS POTENTIAL MECHANISMS FOR DRUG-INDUCED CHOLESTASIS BY AMOXICILLIN AND CLAVULANIC ACID

Diploma thesis

Performed at

UNIVERSITY OF VALENCIA
Faculty of Medicine and Odontology
Joint Research Unit in Experimental Hepatology
Hospital La Fe, Valencia

Supervisors:
Prof. PharmDr. Petr Pávek, Ph.D.
Prof. Ramiro Jover Atienza, Ph.D.

Hradec Králové 2018 **Veronika Řepová**

UNIVERZITA KARLOVA
Farmaceutická fakulta v Hradci Králové
Katedra farmakologie a toxikologie

ZMĚNY GENOVÉ EXPRESE HEPATOBILIÁRNÍCH TRANSPORTÉRŮ JAKO POTENCIÁLNÍ MECHANISMY VZNIKU POLÉKOVÉ CHOLESTÁZY NAVOZENÉ AMOXICILINEM A KYSELINOU KLAVULANOVOU

Diplomová práce

Vypracováno na

UNIVERZITĚ VE VALENCII
Lékařská a odontologická fakulta
Společná výzkumná skupina experimentální hepatologie
Nemocnice La Fe, Valencie

Vedoucí diplomové práce:
Prof. PharmDr. Petr Pávek, Ph.D.
Prof. Ramiro Jover Atienza, Ph.D.

Hradec Králové 2018 **Veronika Řepová**

Declaration

"I declare that this diploma thesis represents my original author work. All literature and other sources used for writing this thesis are summarized in the list of references and cited properly in the text. This diploma thesis was not used in the same or in a similar version to obtain any other academic title."

„Prohlašuji, že tato práce je mým původním autorským dílem. Veškerá literatura a další zdroje, z nichž jsem při zpracování čerpala, jsou uvedeny v seznamu použité literatury a v práci řádně citovány. Tato práce nebyla použita k získání jiného či stejného titulu."

In Hradec Králové, 15.8.2018 ……...

Veronika Řepová

Acknowledgement

I would like to express my great thanks to Prof. Ramiro Jover Atienza, Ph.D. and Prof. Petr Pávek, Ph.D for their professional guidance, consultations, revising the text of this thesis and for enabling this international collaboration. My great thanks also belong to Petar D. Petrov, Ph.D for his guidance, kindness and for showing me all necessities I needed to perform experiments and methods used in this thesis.

Many of my great thanks go to all employees and researchers from Joint Unit of Experimental Hepatology in Hospital La Fe, Valencia, Spain, for their kindness and willingness to help.

Last but not least, I would like to thank to my whole family, my closest friends and my partner Jiří for their patience and endless support during my work on this thesis and through all my university studies.

Thank you all!

ABSTRACT

Charles University

Faculty of Pharmacy in Hradec Králové

Department of Pharmacology & Toxicology

Student: Veronika Řepová

Supervisor: Prof. PharmDr. Petr Pávek, Ph.D., Prof. Ramiro Jover Atienza, Ph.D.

Title of diploma thesis: **Alterations in gene expression of hepatobiliary transporters as potential mechanisms for drug-induced cholestasis by amoxicillin and clavulanic acid**

The combination of amoxicillin and clavulanic acid (AMO/CLA) represents one of the most frequent causes of the idiosyncratic type of drug-induced liver injury (DILI) nowadays. Despite difficulties in diagnosis and causality assessment, the clinical features have already been reported and in most of the cases categorized as cholestatic damages. Number of descriptions of the molecular mechanisms of drug-induced cholestasis has been rising recently and the role of hepatobiliary transporters has turned out to be crucial in the pathogenesis. However, the mechanisms of AMO/CLA-induced DILI at the molecular level still remain indistinct. In order to investigate the hepatotoxic effects of AMO/CLA and AMO alone *in vitro*, HepG2 and human Upcyte hepatocytes were used as hepatocellular models. The mRNA levels of key bile acid (BA) transporters, enzymes and nuclear receptors (NRs) were measured by quantitative real-time polymerase chain reaction. The cytotoxic concentrations of AMO/CLA and AMO were excluded using cell viability tests. Moreover, the protein expression levels of key BA transporters were determined by Western blot analysis and image documentation of cultured cells was provided by digital microscopy. Results evidenced that AMO/CLA caused extensive alterations in gene expression levels of BA transporters, enzymes and NRs, whereas AMO affected tested genes minimally. Specifically, AMO/CLA was able to decrease the mRNA levels of the bile salt export pump (BSEP), which could represent the most significant pro-cholestatic mechanism discovered up to now. On the contrary, the gene and protein expression of a transporter mediating uptake of conjugated BAs, the Na^+-taurocholate co-transporting polypeptide (NTCP), was reduced by AMO/CLA, which could denote a compensatory response to accumulated BAs. Nevertheless, it is anticipated that other additional factors could also be involved in the pathogenesis of cholestasis by AMO/CLA. Therefore, results allow concluding for the first time that AMO/CLA negatively influences the expression of key BA transporters, which could hamper normal bile flow and promote cholestatic DILI.

ABSTRAKT

Univerzita Karlova

Farmaceutická fakulta v Hradci Králové

Katedra farmakologie a toxikologie

Studentka: Veronika Řepová

Školitel: Prof. PharmDr. Petr Pávek, Ph.D., Prof. Ramiro Jover Atienza, Ph.D.

Název diplomové práce: **Změny genové exprese hepatobiliárních transportérů jako potenciální mechanismy vzniku polékové cholestázy navozené amoxicilinem a kyselinou klavulanovou**

Amoxicilin a kyselina klavulanová (AMO/CLA) představují v současné době jednu z nejčastějších příčin idiosynkratického polékového poškození jater (DILI). Navzdory obtížím v diagnostice a vyhodnocování kauzality byly již klinické projevy zdokumentovány a ve většině případů klasifikovány jako cholestatické jaterní poškození. Počet studií týkajících se molekulárních mechanismů polékové cholestázy se stále zvětšuje, přičemž role hepatobiliárních transportérů se ukázala být pro patogenezi zásadní. Molekulární mechanismy vzniku DILI navozeného AMO/CLA však zůstávají stále neobjasněny. Za účelem prozkoumat hepatotoxický efekt AMO/CLA a AMO *in vitro* byly jako hepatocelulární modely použity buňky HepG2 a lidské hepatocyty Upcyte. Hladiny mRNA klíčových transportérů pro žlučové kyseliny (BAs), enzymů a jaderných receptorů (NRs) byly změřeny použitím kvantitativní polymerázové řetězové reakce. Cytotoxické koncentrace AMO a AMO/CLA byly vyloučeny pomocí testů buněčné životaschopnosti. Kromě toho byla exprese důležitých proteinových transportérů pro BAs stanovena Western blot analýzou a obrazová dokumentace kultivovaných buněk byla zajištěna pomocí digitální mikroskopie. Výsledky dokládají, že AMO/CLA způsobil rozsáhlé změny v genové expresi transportérů pro BAs, enzymů a NRs, zatímco samotný AMO ovlivnil expresi testovaných genů minimálně. Kombinace AMO/CLA byla konkrétně schopna snížit mRNA hladinu „bile salt export pump“ (BSEP), což by mohlo představovat doposud nejvýznamnější objevený pro-cholestatický mechanismus. Exprese genu a proteinu transportéru zajišťujícího vychytávání konjugovaných BAs, „Na^+-taurocholate co-transporting polypeptide“ (NTCP), byla naopak díky AMO/CLA snížena, což může představovat kompenzační odezvu na kumulované BAs. Předpokládá se však, že v patogenezi DILI po AMO/CLA mohou být zapojeny i další přídatné faktory. Výsledky proto umožňují dojít k závěru, že AMO/CLA negativně ovlivňuje expresi klíčových transportérů pro BAs, což by mohlo bránit fyziologickému toku žluče a podpořit tak cholestatický typ DILI.

TABLE OF CONTENTS

1 LIST OF ABBREVIATIONS

ABC – ATP-binding cassette

ACTβ – β (Beta)-Actin

AMO – Amoxicillin

AMO/CLA – Amoxicillin/clavulanic acid

AMO/CLA DILI – Amoxicillin/clavulanic acid-induced liver injury

ALT – Alanine aminotransferase

ALP – Alkaline phosphatase

APS – Ammonium persulphate

BA(s) – Bile acid(s)

BSA – Bovine serum albumin

BSEP – Bile salt export pump

BSH – Bile salt hydrolase

C_{max} – Maximum plasma concentration

CA – Cholic acid

CDCA – Chenodeoxycholic acid

cDNA – Complementary deoxyribonucleic acid

CIOMS – The Council for International Organizations of Medical Sciences

CLA – Clavulanic acid (clavulanate)

CYP – Cytochrome P450

DCA – Deoxycholic acid

DDI H_2O – Distilled and deionized water

DILI – Drug-induced liver injury

DILIN – Drug-induced liver injury network

DMSO – Dimethyl sulfoxide

dNTPs – Deoxyribonucleotide triphosphates

DTT – Dithiothreitol

EDTA – Ethylenediaminetetraacetic acid

FDA – Food and drug administration

FXR – Farnesoid X receptor

GABA – γ (Gamma)-aminobutyric acid

GAPDH – Glyceraldehyde 3-phosphate dehydrogenase

GPCR(s) – G-protein coupled receptor(s)

HLA – Human leukocyte antigen

HMGCR – 3-Hydroxy-3-methylglutaryl coenzyme A reductase

IL-6 – Interleukin 6

logP – Octanol-water partition coefficient

LCA – Lithocholic acid

LXR – Liver X receptor

MDR(s) – Multidrug resistance protein(s)

M-MLV – Moloney-Murine leukemia virus

MRP(s) – Multidrug resistance-associated protein(s)

MTT – Methylthiazolyldiphenyl tetrazolium bromide

mRNA – Messenger ribonucleic acid

NAPQI – N-acetyl-*p*-benzoquinone imine

NTCP – Sodium taurocholate co-transporting polypeptide

OA^- – Organic anions

OATP – Organic anion transporting polypeptide

OD – Optical density

Oligo dT – Oligo deoxy-thymidine

OST – Organic solute and steroid transporter

PBGD – Porphobilinogen deaminase

PBP(s) – Penicillin-binding protein(s)

PBS – Phosphate-buffered saline

PVDF – Polyvinylidene difluoride

q-RT-PCR – Quantitative real-time polymerase chain reaction

SDS – Sodium dodecyl sulphate

SDS-PAGE – Sodium dodecyl sulphate polyacrylamide gel electrophoresis

SHP – Small heterodimer partner

SLC – Solute carrier

TAE buffer – Tris-acetate-EDTA buffer

TBS – Tris-buffered saline

TE buffer – Tris-EDTA buffer

TEMED – Tetramethylethylenediamine

TNFα – Tumor necrosis factor α

ULN – Upper limits of normal of serum alanine aminotransferase/alkaline phosphatase

VALP – Valproic acid (valproate)

2 INTRODUCTION

Drug-induced liver injury (DILI) represents a group of hepatic damages caused by exposure to certain registered medicines as well as to certain dietary supplements and herbal preparations. Among registered drugs, the antibacterially active combination of amoxicillin (AMO) and clavulanic acid (CLA) was found to be the most frequent cause of idiosyncratic type of DILI in the United States of America (Chalasani et al. 2008), Spain (Andrade et al. 2005) and Iceland (Björnsson et al. 2013).

Most cases of amoxicillin/clavulanic acid-induced liver injury (AMO/CLA DILI) show symptoms of cholestatic damage, and the typical clinical features and risk factors of this hepatotoxicity have been described during the last years (deLemos et al. 2016, Lucena et al. 2006, Robles et al. 2010). However, the presentation of AMO/CLA-induced cholestasis consists of several nonspecific syndromes such as jaundice and bile duct injury accompanied by altered liver tests, thus the differential diagnosis is very difficult. Moreover, a delayed outbreak of symptoms and a widespread polypragmasy represent another diagnostic complication (deLemos et al. 2016).

It is well-known that cholestasis is caused by reduced bile secretion from hepatocytes or obstruction of the biliary transport system. The mechanisms of drug-induced cholestasis at the molecular level have been at the centre of interest for the last decades. The understanding of functions and alterations in transporters located at the basolateral and canalicular membranes of hepatocytes helps to clarify the principles of cholestasis. In this regard, two main transporters, the Na^+-taurocholate co-transporting polypeptide (NTCP) important for bile acids uptake and the bile salt export pump (BSEP) crucial for bile acids efflux from hepatocytes, have been widely investigated. Specifically, a reduction of NTCP and BSEP expression by cholestatic drugs was observed to be an important mechanism for cholestatic injury (Byrne et al. 2002, Dawson et al. 2009, Zollner et al. 2001). However, the whole process seems to be more complex with the contribution of several factors (Wagner et al. 2009).

A better understanding of DILI pathogenesis and cholestatic mechanisms of AMO/CLA could help to improve prevention, diagnosis and treatment of this pathological condition. For this purpose, the effect of AMO/CLA on gene expression of representative hepatobiliary transporters, enzymes and nuclear receptors involved in bile acid synthesis, homeostasis and transport will be evaluated in this experimental diploma thesis.

3 THEORETICAL PART

3.1 The drugs of interest

The drugs of interest, **amoxicillin and clavulanic acid**, are frequently used antibacterial agents which are commonly prescribed in combination (in the Czech Republic known as *Amoksiklav*®, *Augmentin*®, *Betaklav*® and *Medoclav*®) or as amoxicillin alone (in the Czech Republic known as *Duomox*® and *Ospamox*®).

The **routes of administration** are variable. It is common to use these remedies in the form of either tablets and suspensions administered orally or solutions for injection and infusion. Amoxicillin is an acid-stable substance and its absorption is not influenced by food when administered orally (Brunton et al. 2011).

As mentioned above, amoxicillin and clavulanic acid are antibacterial agents effective against a wide range of bacteria (including mainly Gram-positive, but also Gram-negative groups). From a clinical point of view, these drugs are ordinarily used to treat **bacterial infections** such as respiratory tract infections, sinusitis, inflammation of the middle ear, urinary tract, skin, soft tissue, bone and joint infections. Last but not least, amoxicillin can be prescribed in combination with other antibacterial chemotherapeutics and proton pump inhibitors to eradicate *Helicobacter pylori* when causing gastric ulcers (Brunton et al. 2011, Lüllmann et al. 2002).

3.1.1 Amoxicillin

Amoxicillin (*Amoxicillinum*) is a semi-synthetic broad-spectrum antibacterial medicine which belongs to the **penicillins**. The penicillins constitute a large group of antibacterially active compounds which counts among the β-lactam class of antibiotics together with cephalosporins, carbapenems and monobactams (Brunton et al. 2011).

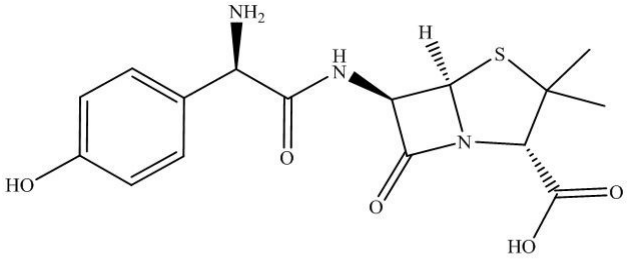

Figure 1 ***The structure of amoxicillin***

As is well known, the beginning of this famous antibiotic family is dated to 1928 when Sir Alexander Fleming discovered the antibacterial activity of certain

ascomycetous fungi, *Penicillium chrysogenum*[1]. He found out that a product of this mould can inhibit the growth of *Staphylococcus* Gram-positive bacteria by an accident (Brunton et al. 2011, Hollinger 2003).

Fleming's discovery was hidden in the shadow until an Australian pharmacologist Howard Florey and a German biochemist Sir Ernst Chain started to study the isolation of this compound responsible for antibacterial activity in the 1940s (Hollinger 2003). In 1945, Sir Alexander Fleming, Howard Florey and Sir Ernst Chain were awarded the Nobel Prize for Physiology or Medicine for their contribution to the treatment of infectious diseases. The leading compound, penicillin, was discovered as well as methods for purification and ways of production for clinical use. This exceptional event of discovery in 1928 transformed the way how bacterial infections are treated and from 1942 has saved plenty of lives especially during the Second World War, when the clinical use started (Rifkind and Freeman 2005).

All penicillins share a β-lactam ring connected with a thiazolidine ring. These two rings form the main skeleton called **6-aminopenicillanic acid**. The difference between every active pharmaceutical substance among penicillins is seen in the acylamino side chain attached to the main skeleton (Brunton et al. 2011). The structural formula of AMO can be seen in Figure 1. There is a hydroxyl group in para position on the side phenyl ring, and thus AMO is also called 4-hydroxy-ampicillin. The molecular weight is 365.404 g/mol and molecular formula looks as follows: $C_{16}H_{19}N_3O_5S$ (PubChem 2017a).

The structure of β-lactam ring plays a key role for **mechanism of antibacterial activity**. The β-lactam ring inhibits the formation of peptidoglycan cross-links in bacterial cell walls by covalent binding to the **penicillin-binding proteins** (PBPs). PBPs are proteins responsible for the formation and maintenance of peptidoglycan cell wall which is very important for viability of the bacteria. This fact results in damages of newly synthesized cell walls which in fact raises the permeability of cell walls and so bacteria are fated to death. That means the penicillins are bactericidal compounds (Brunton et al. 2011).

The drug of interest, amoxicillin, belongs together with ampicillin to the subgroup called **aminopenicillins**, modern semi-synthetic compounds with extended antibacterial spectrum effective against Gram-positive and Gram-negative bacteria.

[1] Formerly termed *Penicillium notatum* (Hollinger 2003)

Another advantage of aminopenicillins is seen in their stability in acidic conditions and gastrointestinal tract. AMO was designed to be better absorbed from the intestines in comparison with ampicillin. The absorption of AMO is almost twice higher even after alimentation which results in smaller amount of adverse gastrointestinal side effects (Lüllmann et al. 2002).

When talking about **adverse effects** of AMO, it is necessary to mention the typical group side effect – allergy to penicillins. The symptoms of this allergic reaction include high temperature or fever, itchiness, rash, angioedema or even an anaphylactic shock. The β-lactam ring can be metabolically broken down to form penicilloic acid which is reactive with tissue proteins and constitutes the antigenic agents. The serious condition of anaphylactic shock can be laboratory detected by elevated levels of specific IgE antibodies in patient's blood (Bennett et al. 2012). Patients with allergy to penicillins should give a notice about this problem to their doctors or pharmacists. Another adverse effect resulting from the antibacterial action is diarrhoea on the basis of disrupted physiological intestinal microflora among sensitive patients. Another important adverse effect is hepatotoxicity. A textbook of pharmacology reports hepatotoxicity (specifically cholestatic jaundice) after the use of AMO/CLA in elderly individuals when using these medications for a prolonged period in higher doses (Bennett et al. 2012). Moreover, cases of idiosyncratic hepatic injury after exposure to AMO alone, but mostly in the combination with CLA, have been uncovered in the last decades (deLemos et al. 2016, Robles et al. 2010).

One of the consequences that follows from the widespread use of antibacterial agents is the development of drug **resistance** among particular pathogens, e.g. bacterial genus *Staphylococcus*. The mechanism of resistance is mediated by β-lactamases, bacterial enzymes able to hydrolyse β-lactam ring, thus the drug loses its antibacterial activity (Clark et al. 2012). On the grounds of this fact, **β-lactamase inhibitors** were developed to prevent the inactivation of antibacterial drugs and are administrated together with amoxicillin or ampicillin, to give an example (Brunton et al. 2011).

3.1.2 Clavulanic acid

The second studied remedy is **clavulanic acid** (*Acidum clavulanicum*), a member of **β-lactamase inhibitors** often used with amoxicillin under the name

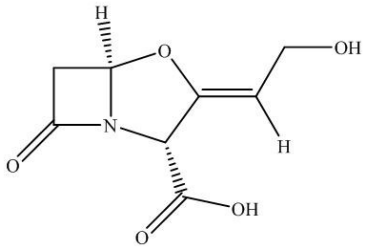

Figure 2 ***Clavulanic acid***

co-amoxiclav. Clavulanic acid is usually formulated into pills as potassium clavulanate (*Kalii clavulanas*), a salt representing 62.5 mg or 125 mg of CLA in one tablet given orally, or 100 mg of CLA in 10 mL of intravenous injection solution. The β-lactamase inhibitors are strictly administrated together with antibacterial drugs which are not active against organisms producing β-lactamases, specifically penicillinase. *Staphylococcus aureus*, *Enterobacter, Neisseria gonorrhoeae* or *Klebsiella pneumoniae* are categorized among these problematic bacteria species (Lüllmann et. al 2002).

The structure of β-lactamase inhibitors is similar to the structure of penicillins, therefore the **mechanism of action** follows an analogous pathway. It contains a β-lactam ring which is opened by bacterial enzymes preferentially. However, the β-lactamase inhibitory activity appears when the inhibitor irreversibly bounds to the enzyme once the ring has been opened, thus leading to enzyme inactivation. It is necessary to have on mind that inhibitors of β-lactamases do not have own antibacterial activity (Lüllmann et al. 2002).

The structural formula of CLA is shown in Figure 2. The molecular weight is 199.162 g/mol and molecular formula looks as follows: $C_8H_9NO_5$ (PubChem 2017b).

3.1.3 Valproic acid

Valproic acid *(Acidum valproicum)* is a very important antiepileptic drug. The structural formula of VALP, dipropylacetic acid, can be seen in Figure 3. The molecular weight is 144.214 g/mol and molecular formula looks as follows: $C_8H_{16}O_2$ (PubChem 2017c). The substance is usually used as potassium or sodium salt in therapeutic formulations.

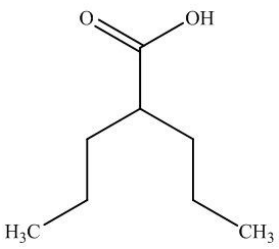

Figure 3 ***Valproic acid***

The **mechanism of anticonvulsant action** is complex and inhomogeneous. Firstly, it includes an increase in γ-aminobutyric acid (GABA), the main inhibitory substance in the central nervous system. Secondly, valproic acid (VALP) keeps Na^+ channels in inactivated state, thirdly, inactivation of T-type Ca^{2+} channels is present as well (Brunton et al. 2011).

The main **adverse effects** involve gastrointestinal problems such as nausea with or without vomiting, stimulation or absence of appetite and central nervous system effects such as sedation or tremor. The adverse effect of our interest is hepatotoxicity

manifested as increased levels of hepatic transaminases, hepatitis, cholestasis and mainly steatosis (Brunton et al. 2011). The steatohepatitis was recorded for the first time in the early 1980s and the start of its therapeutic use is commonly dated on 1969 in France and nine years later in the United States of America (Zimmerman and Ishak 1982). On the grounds of these findings, the mechanism of steatosis was investigated in animal models and liver-derived cell models. It is supposed that the inhibition of fatty acids β-oxidation by preferentially forming valproyl-coenzyme A metabolite is a principal mechanism of steatosis (Silva et al. 2001).

This drug was used in the form of **sodium valproate** as a control substance with proven hepatotoxicity (mainly steatosis), and its ability to cause alterations in gene expression levels of hepatic bile acid transporter was confirmed (Donato et al. 2016).

3.2 Drug-induced liver injury

3.2.1 Definition, characteristics and incidence

Drug-induced liver injury is defined as damage to the liver that is unequivocally elicited by drugs or herbal remedies that leads to biochemical liver test alterations or liver dysfunction, while exclusion of other possible aetiologies is necessary. More than 1 000 drugs and toxins are included on the list of suspected causal agents inducing liver damages, but causality is proven only for a drop of them. It was also reported that DILI may account for approximately 5 % of all admissions to the hospital, 10 % of all cases of acute hepatitis, and 50 % of all acute liver failures (Hillman et al. 2016, Singh et al. 2016). Moreover, it was enumerated that DILI develops in 1 in 100 patients when receiving medications during hospitalisation (Meier et al. 2005).

DILI can be characterized as **intrinsic** (adverse effect type A, predictable), typical for paracetamol (acetaminophen) with its metabolite N-acetyl-*p*-benzoquinone imine (NAPQI), or **idiosyncratic** (adverse effect type B, unpredictable), typical for drugs of interest in this thesis (Leise et al. 2014). Most of the harmful hepatic reactions are idiosyncratic (Hussaini and Farrington 2007) and widely depend on the susceptibility of exact host's metabolic, immune and genetic predispositions (Andrade et al. 2004). Current studies during preclinical phases of drug development do not predict idiosyncratic DILI satisfactorily and that is why idiosyncratic DILI represents the major cause for drug failure in premarketing and also postmarketing phases when accounts for up to 29 % of all drug withdrawals from the market (Lee 2013).

DILI is a hepatotoxicity which can be caused by certain registered medications (on prescription or over-the-counter), but even by dietary supplements and herbal preparations. For instance, in Spain and France the most observed causes of DILI are specific anti-infectious drugs (such as amoxicillin/clavulanic acid), hypolipidemic, psychotropic, antidepressant and non-steroidal anti-inflammatory agents (Andrade et al. 2005, Sgro et al. 2002). Furthermore, the combination of AMO/CLA is the leading cause, but other anti-infectious drugs (such as nitrofurantoin and isoniazid), central nervous system agents, immunomodulatory and non-steroidal anti-inflammatory drugs are other significant causes of DILI in the United States of America (Chalasani et al. 2008).

In previous population-based studies, the **crude incidence of DILI** was estimated. In a population-based study from France, the incidence of 13.9 cases among 100 000 persons per year was described (Sgro et al. 2002). Another similar study from Iceland, estimated the annual crude incidence to be 19.1 cases per 100 000 persons (Björnsson et al. 2013).

Despite the relatively low incidence, DILI is a problem which affects many fields of the health care system. The preclinical and clinical developments of new drugs, patients, doctors, and last but not least the regulatory system of drug safety are influenced by this phenomenon (Watkins and Seeff 2006). Currently, acute liver injury developed by drugs is one of the most serious problems in pharmacovigilance and the leading cause of drugs' withdrawal from the market as postulated in a study including data from the United Kingdom, United States of America and Spain (Bakke et al. 1995).

Not only pharmaceutical industry, but more patients' health is at stake. On the basis of these concerns, novel **predictive biomarkers** (for instance, circulating organ-specific microRNAs) for early discovery of potentially hepatotoxic drugs even during drug development are in the interest of current studies (López-Riera et al. 2017, Starkey Lewis et al. 2011, Wang et al. 2009). Namely, the liver-specific microRNA-122 could be a promising biomarker for early diagnosis of AMO/CLA DILI (Lee et al. 2017).

3.2.2 Classification

Classification of DILI based on type of adverse response

DILI is a group of hepatic damages and one of the easiest classifications is established on the grounds of general types of drugs' adverse effects. Two categories of drugs' adverse effects can be seen in drug-induced liver diseases. The **intrinsic** DILI

which is predictable, typical for paracetamol, and the **idiosyncratic** DILI which is unpredictable, typical for drugs as specific antibiotics and nonsteroidal anti-inflammatory drugs (Leise et al. 2014). These idiosyncratic drugs' reactions are not possible to predict on the basis of information about dosage and therapeutic effect.

Classification of DILI based on biochemical and histological parameters

The main classification of DILI was established on the basis of histological patterns and hepatic enzymes alterations. First type of DILI is called **hepatocellular**, also known as hepatic or hepatitis-like, second type is called **cholestatic** and third type is a connection of those mentioned above and is called **mixed** type of DILI (Bénichou 1990).

- **Hepatocellular type**

In hepatocellular cases, prevailing cytolytic damage of hepatocytes by apoptosis or necrosis results in higher level of serum transaminases even before jaundice appears (Abboud and Kaplowitz 2007).

- **Cholestatic type**

Cholestasis is defined as the impairment of normal bile flow with the concomitant accumulation of bile acids in the liver or in the systemic circulation, resulting from either a functional defect at the hepatocyte level (hepatocellular bile secretion) or obstruction at the bile duct level (interlobular ducts or ductules). Cholestatic type DILI is characterized by cholestasis due to the direct harmful effect of a drug or its toxic metabolites, but the cause can also stand on the side of adaptive immune response of a host body (Abboud and Kaplowitz 2007). It is important to mention jaundice and bile duct injuries as typical clinical syndromes, although these are very unspecific (Mohi-ud-din and Lewis 2004).

For a long time, there was a need for accurate characterization of DILI and its causality assessment. Therefore, the Council for International Organizations of Medical Sciences (CIOMS) in 1990 prepared biochemical criteria of evaluation and described mentioned pathophysiological conditions (Bénichou 1990). The criteria of diagnosis undertook some modifications made by Food and Drug Administration (FDA) and the main assessing hallmark was settled to be the **R ratio** (ratio of serum alanine aminotransferase to the alkaline phosphatase, according to their upper limits of normal – ULN) (Danan and Bénichou 1993).

The classification of DILI types using mentioned biochemical parameters and CIOMS scale is summarized in Table 1:

Table 1 ***Classification of DILI based on biochemical parameters***

	Hepatocellular type	**Cholestatic type**	**Mixed type**
Formula and value of the R ratio	$\frac{(\frac{ALT}{ULN})}{(\frac{ALP}{ULN})} \geq 5$	$\frac{(\frac{ALT}{ULN})}{(\frac{ALP}{ULN})} \leq 2$	$2 \leq \frac{(\frac{ALT}{ULN})}{(\frac{ALP}{ULN})} \leq 5$
The level of main hepatic enzyme	ALT ≥ 3 ULN	ALP ≥ 2 ULN	ALT > 3 ULN ALP > 2 ULN

Explanatory notes: ALT – Alanine aminotransferase; ALP – Alkaline phosphatase; ULN – Upper limits of normal
Modified according to: Danan and Bénichou 1993

It is important to be aware of many pitfalls of this classification. Firstly, there is no recommended time period when the biochemical tests should be performed (Leise et al. 2014). Some population-based study showed different proportional representation of each DILI type in the same patients depending on whether tests are performed at the time of diagnosis or later during the progress of injury (Fontana et al. 2010). Secondly, DILI by the same drug can be characterized by different biochemical values in different patients (Leise et al. 2014).

3.2.3 Risk factors

The risk factors for DILI are not still firmly characterized. In general, it is possible to reach an agreement about the influence of **gender, age, comorbidities, genetic predispositions and exposure to specific drugs** on development DILI (Lucena et al. 2009). The problem of enumerating all risk factors consists in lack of available empiric data and difficulties in causality assessment (Leise et al. 2014).

Following the main classification of DILI, hepatocellular type is usually seen among younger females, while cholestatic and mixed type is often observed in older males. The trend for developing cholestatic DILI was reported mostly in patients older than 60 years (deLemos et al. 2016, Lucena et al. 2009). Regarding AMO/CLA DILI, the group of patients with the highest risk are men with advanced age (deLemos et al. 2016).

Although the idiosyncratic type of DILI is commonly thought not to be dose-dependent, in the study using databases from the United States of America and Sweden, a certain connection between high daily doses (higher than 50 mg per day) and hepatotoxicity was observed in a US and a Swedish group. In a Swedish group, the medicines with daily dose higher than 50 mg accounted for 77 % of all grave DILI cases (Lammert et al. 2008). Some years later, combined aspects of daily dosage and drug's lipophilicity were observed. A strong connection was found between daily dosage higher than 100 mg and high drug lipophilicity expressed as octanol-water partition coefficient (log P) ≥ 3 (Chen et al. 2013).

Another risk factor can be hidden in genetic code. Small modifications in human leukocyte antigen (HLA) class II are connected with a variety of diseases and immune-mediated responses to drugs. HLA molecules play a key role in immune system and in presentation of antigens. To be more specific, idiosyncratic cholestatic or mixed cases of DILI after AMO/CLA exposure were linked with HLA-DRB1*1501 and HLA-DQB1*0602 alleles in the previous study (Donaldson et al. 2010).

3.2.4 Diagnosis

The clinical manifestation of DILI is not uniform and strongly depends on the causal agent and host's predisposition. In general, clinical DILI manifestations are very similar to other liver diseases, for instance: non-alcoholic fatty liver disease, alcoholic hepatitis, obstructive cholestasis etc. That is the reason why diagnosis is very difficult and evaluation of many other possible liver diseases with precise differential diagnosis is needed. An accurate DILI diagnosis requires careful causality assessment, compatible clinical and laboratory features, and the exclusion of alternative root causes, as long as there is no objective testing method for making the diagnosis and no firmly estimated agreement on patterns for different types of DILI (Leise et al. 2014).

The diagnosis strongly relies on doctor's experiences and completeness of information about the patient's medical history (Fontana et al. 2010). Another situation that makes the diagnosis more difficult is polypragmasy which occurs very often. Nowadays, when patients take many different remedies (prescribed, over-the-counter or even the food supplements) it is not easy to assign causation to a single medicine. Moreover, the combination of specific drugs can sometimes works in a different way than each medicine alone (Leise et al. 2014).

Certainly, the proved usage of suspected remedy is necessary for the diagnosis of DILI, but especially in idiosyncratic DILI the **latency period**[2] is significantly long and complicates the causality assessment. The latency period of DILI in general varies from days up to 1 year (Leise et al. 2014).

DILI is usually manifested by variable symptoms, for instance: nausea, malaise, vomiting, abdominal pain, itching and jaundice. Total clinical features of the disease vary from banal alterations of hepatic enzymes to severe liver dysfunctions or even acute liver failure which can end up in liver transplantation. Most common clinical symptoms are alterations in levels of main hepatic enzymes, such as alanine aminotransferase (ALT) and alkaline phosphatase (ALP), and accumulation of conjugated bilirubin and bile acids in hepatocytes or in the systemic blood. Abnormally high accumulation of bile acids in hepatocytes is dangerous. If the concentration of bile acids exceeds the maximum binding capacity of the cytosolic binding proteins in hepatocytes, bile acids will initiate necrosis and apoptosis within hepatocytes (Palmeira and Rolo 2004).

3.2.5 Amoxicillin/clavulanic acid-induced liver injury

The importance of staying focused on **amoxicillin/clavulanic acid-induced liver injury** is supported by statistical information. According to the Drug-Induced Liver Injury Network (DILIN), the research group of specialists in the USA, AMO/CLA is the leading cause of idiosyncratic DILI in the USA (Chalasani et al. 2008). Another group of scientists from Spain published the same results about AMO/CLA as the most frequently observed cause of idiosyncratic DILI (Andrade et al. 2005). It is also worth to notice the prospective study from Iceland, the island in the North Atlantic Ocean with population of around 251 000 residents (of age 15 and more). Due to cooperation with general practitioners and gastroenterologists all around the country, the cases of liver injuries feasibly caused by drugs, herbal and dietary supplements were examined. During the tested period of 2 years (2010-2011), 96 patients were diagnosed with DILI and the combination of AMO/CLA was identified as the most frequently involved agent (21 patients from 96 total) in this health issue (Björnsson et al. 2013).

---

[2] **Latency period** = the time interval between initiation of drug usage and symptom onset determined by DILI diagnosis (Leise et al. 2014)

The most significant **clinical characteristics** of AMO/CLA DILI were collected in the US DILIN registry (deLemos et al. 2016) and compared with other antimicrobial medications these characteristics can be described as follows: the average age in patients with AMO/CLA DILI was 60 years, which was considerably higher than the average age of 48 years in patients using other antimicrobials, the male gender represented a substantial proportion (62 %) of all AMO/CLA cases, the average latency period was calculated to last from 16 days (Lucena et al. 2006) to 29 days (deLemos et al. 2016) and jaundice was developed in more than 80 % of patients with AMO/CLA DILI (deLemos et al. 2016, Lucena et al. 2006).

When talking about DILI classification, it is important to note that the **cholestatic type** was presented as the most predominant type among all diagnosed AMO/CLA DILI cases (deLemos et al. 2016, Lucena et al. 2006, Robles et al. 2010).

3.3 Bile acids

In human body, bile acids (BAs) are not only important to facilitate digestion and absorption of lipids and certain nutrients and compounds (such as fat-soluble vitamins) in the small intestine, but also for the biliary excretion of endogenous steroids (such as cholesterol), many xenobiotics (e.g. phenytoin and cyclosporine A) and their metabolites (Chiang 2013). Another bile acids' key role is to act as signalling molecules which activate certain nuclear receptors (NRs) and several G-protein coupled receptors (GPCRs) in order to regulate metabolic processes in digestive system and whole human body, as well as represent adaptive responses in the hepatic tissue and other tissues to avoid toxicity caused by BAs (Chiang 2013, Chiang 2017).

The synthesis, metabolism and transport of BAs are complex processes regulated by many BA transporters, NRs and enzymes. Changes against the balanced state cause liver diseases (e.g. cholestasis, steatosis and fatty liver disease), hepatic inflammation and dyslipidaemia, which in turn can lead to cardiovascular diseases. According to this, the homeostasis of BAs needs to be maintained for the healthy human organism (Chiang 2013).

3.3.1 Chemical properties

From a chemical point of view, BAs represent a group of amphipathic molecules synthesized in human liver as final products of cholesterol metabolism. The basic chemical structure is **cholanoic acid** (C_{24}-5β-bile acid) with steroid sterane nucleus. The sterane nucleus contains four fused carbon rings (one cyclopentane ring and three cyclohexane rings) with several substitutions of hydroxyl and methyl groups. Each BA has α-configuration of 3-hydroxyl group, β-configuration of 5-hydrogen and *cis*-configuration of fused A and B rings (Chiang 2013).

At the physiological pH, BAs are presented as anions and that is why terms "bile acids" and "bile salts" are commonly used as equivalents in the literature (Schaap et al. 2013).

3.3.2 Bile acids synthesis

In general, the synthesis of BAs starts with the synthesis of cholesterol. For this important metabolic pathway the rate-limiting enzyme is the **3-hydroxy-3-methylglutaryl-coenzyme A reductase (HMGCR)** which mediates the synthesis of mevalonic acid from 3-hydroxy-3-methylglutaryl-CoA (Brunton et al. 2011).

Generally, two major pathways of *de novo* BA synthesis from cholesterol are known in human liver. In both ways, the primary bile acids called **cholic acid (CA)** and **chenodeoxycholic acid (CDCA)** are formed within hepatocytes (Chiang 2013).

Classic biosynthetic pathway

The classic biosynthetic pathway is characterized by initiation due to rate-limiting enzyme **cholesterol 7α-hydroxylase (CYP7A1)**. When microsomal enzyme **sterol 12α-hydroxylase (CYP8B1)** is present, the final product of synthesis is CA. When this last mentioned enzyme is missing, the final product is CDCA (Chiang 2013).

Alternative biosynthetic pathway

Second major way of biosynthesis, the alternative pathway (also called acidic), is started by mitochondrial **sterol 27-hydroxylase (CYP27A1)**. Enzyme CYP27A1 can be found in macrophages and most of the human tissues. The next step of this pathway requires **oxysterol and steroid 7α-hydroxylase (CYP7B1)**, which is expressed in macrophages, liver and tissues with steroidogenic activity (Chiang 2013).

After *de novo* synthesis, primary BAs are largely conjugated with amino acids, namely **glycine** and **taurine**, or form salts. These forms of BAs are secreted via transporters of canalicular membrane from hepatocytes into the bile, which is stored and concentrated in the gallbladder. The fact of conjugation and formation of sodium salts is important for increasing of solubility at the physiological pH and decreasing passive absorption (Chiang 2013).

3.3.3 Enterohepatic circulation and excretion of bile acids

Briefly, BAs are synthesized in the liver and secreted with the bile, which flows into the small intestine to participate in digestive processes. The BA reabsorption from the intestines is a very important step for maintaining BA homeostasis (Chiang 2013).

The majority of BAs are reabsorbed in the small intestine. Several transporters, but also passive diffusion, provide the transport across the enterocytes. Small amount of BAs are reabsorbed in the large intestine, specifically in the colon. In the large intestine, microbiota is essential for the subsequent fate of BAs. There are two important microbial enzymes which have to be mentioned. First, the microbial **bile salt hydrolase (BSH)** causes deconjugation of glyco- and tauro- BAs. Second, due to the **7α-dehydroxylase** activity of intestinal bacteria, the secondary bile acids **deoxycholic acid (DCA)** and **lithocholic acid (LCA)** are produced from deconjugated CA and CDCA, respectively (Chiang 2017).

After the digestive processes, almost 95 % of deconjugated BAs are recycled by reabsorption (Chiang 2013). This enterohepatic circulation is undergone by the majority of CAs, CDCAs and deoxycholic acids. The rest of BAs are excreted via faeces (Chiang 2009). Once absorbed, BAs are secreted into the portal blood and circulated towards hepatocytes. The reabsorption of BAs and their delivery into the liver trigger a significant inhibition of *de novo* BA synthesis and serve as a feedback regulation (Chiang 2017).

3.3.4 Regulation of bile acid homeostasis

The regulation of BA homeostasis is kept by several mechanisms, including negative feedback regulation and inhibition or induction of expression of specific genes encoding transporters, enzymes and NRs participating in BA synthesis, metabolism and transport (Chiang 2009).

One of the regulatory mechanisms is the activation of **farnesoid X receptor (FXR)** by BAs, mostly CDCA. FXR, also known as NR1H4, is a nuclear receptor functioning as a transcription factor. FXR activates transcription of another atypical nuclear receptor, **small heterodimer partner (SHP)**, which in turn stops transcription of important enzymes for BA synthesis – CYP7A1 and CYP8B1. This biochemical pathway symbolizes the negative feedback of BAs (Chiang 2002, Chiang 2017, Goodwin et al. 2000). Another consequence of FXR activation is the increased expression of **uridine 5'-diphosphate glucuronosyl transferase family 2 member B4 (UGT2B4)**. This enzyme mediates the process of glucuronidation – allocation of a glucuronosyl group to hydrophobic BAs which results in increased hydrophilic properties and easier elimination from the body (Barbier et al. 2003). It was also reported that BA-activated FXR with subsequent induction of SHP can repress gene expression of NTCP in rat primary hepatocytes (Denson et al. 2001).

On the other hand, the activation of nuclear receptor **liver X receptors α and β (LXR α and β),** also known as NR1H3 and NR1H2, with oxysterols (oxidized metabolites of cholesterol) leads into the induction of CYP7A1 gene transcription in mice which converts excessive cholesterol into BAs (Lehmann et al. 1997). Another function of LXR, which was seen in mice, is the ability to promote expression of ATB-binding cassette family members G5 and G8 transporters (ABCG5 and ABCG8), but the function in humans is still elusive (Chiang 2002).

3.4 Bile acid transporters

The most important contributor in maintaining BA homeostasis is the **hepatocyte**. Hepatocytes are polarized cells. Two specialized membranes are present: **basolateral (sinusoidal)** membrane and **canalicular (apical)** membrane. Both of these membranes are characterized by specific BA transporters (Figure 4) which help to keep the right balance of BAs in the human body (Chiang 2013, Dawson et al. 2009).

For efficient reuse of BAs, circulating BAs in the portal blood are transported through the basolateral membrane into the hepatocyte, where they can be efflux via the canalicular membrane into the bile canaliculi. Both processes of transport and *de novo* biosynthesis have to be in balance, otherwise pathological conditions such as cholestasis could develop (Dawson et al. 2009).

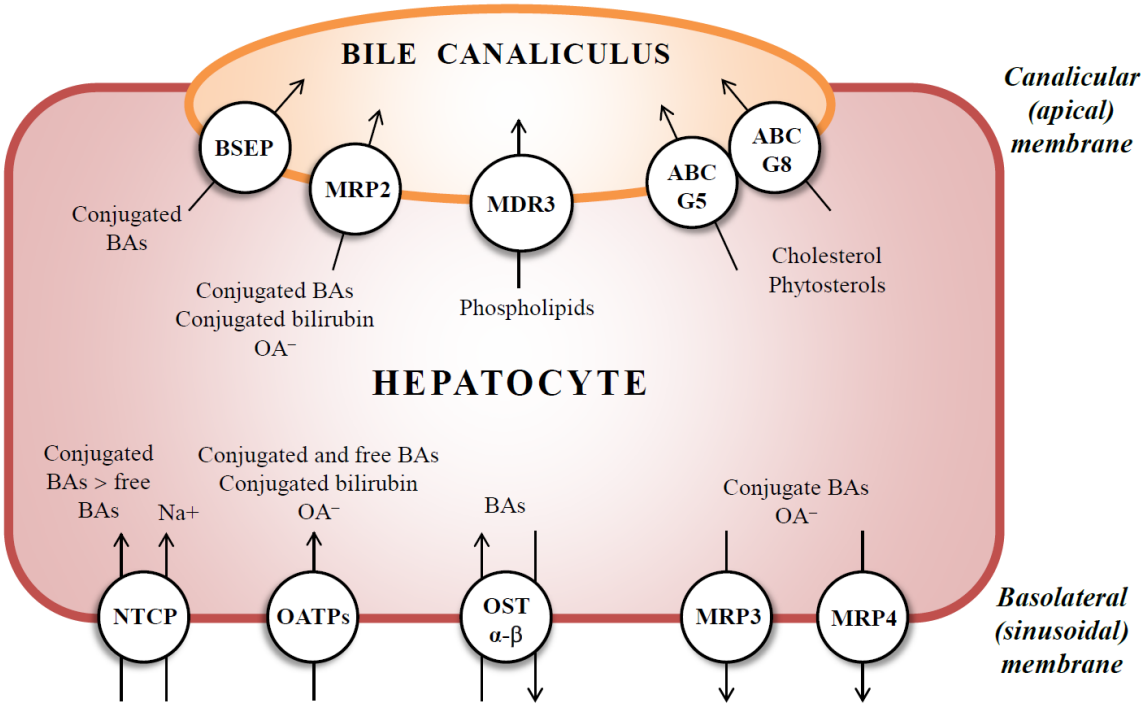

Figure 4 ***Schematic illustration of bile acid transporters at basolateral (sinusoidal) and canalicular (apical) membrane of hepatocyte.*** *Explanatory notes*: ABCG5/8 – ATP-binding cassette G5/8; BAs – Bile acids; BSEP – Bile salt export pump; MDR3 – Multidrug resistance protein 3; MRP2/3/4 – Multidrug resistance-associated protein 2/3/4; NTCP – Na^+-taurocholate co-transporting polypeptide; OA^- – Organic anions; OATPs – Organic anion transporting polypeptides; OST α-β – Organic solute and steroid transporter α-β.

3.4.1 Hepatobiliary basolateral transporters

The basolateral transporters allow communication between hepatocytes and portal blood. There are transporters essential for intake of BAs and other compounds, but other basolateral transporters can support efflux of BAs or other substances from cells towards portal circulation (Dawson et al. 2009).

Sodium taurocholate co-transporting polypeptide

One of the most important transporters for enterohepatic circulation, the **Na^+-taurocholate co-transporting polypeptide** with human gene name **SLC10A1**, performs the largest proportion of uptake of conjugated BAs (namely conjugates with glycine or taurine) but also free BAs into the hepatocytes. This transporter is located at the basolateral membrane of hepatocytes and collects BAs from portal blood to reuse them again in bile. Specifically, NTPC is a membrane glycoprotein with several transmembrane domains (Hagenbuch and Dawson 2004, Hagenbuch and Meier 1994).

The transport by NTCP is described as Na^+-mediated and electrogenic uptake. The main power for the transport is the negative intracellular potential and last but not least inwardly directed Na^+ gradient kept by the basolateral Na^+/K^+-ATPase (Hagenbuch and Dawson 2004).

Organic anion transporting polypeptides

Next transporters involved in BA intake belong to the **solute carrier family SLC01** and are named **organic anion transporting polypeptides (OATPs)**. Specifically, the **OATP1 and OATP2** are Na^+-independent transporters located at the basolateral membrane of hepatocytes. The substrates transported via OATP2 are various, for instance BAs, neutral and conjugated steroids, hormones, organic anions or several xenobiotics; and that is the reason why OATPs perform only a modest function in BA uptake (Chiang 2013, Mikkaichi et al. 2004).

Multidrug resistance-associated proteins

To complete the information about transporters involved in efflux of conjugated BAs, it is important to mention the **multidrug resistance-associated proteins (MRPs)** family, specifically its members with high expression in liver tissue. This family belongs to a numerous and diverse group called ATP-binding cassette (ABC) transporters. At the canalicular membrane located **MRP2**, with the human gene name **ABCC2**, and at the basolateral membrane expressed **MRP3/4**, with the gene name **ABCC3/4**, are very important for BA homeostasis (König et al. 1999).

The basolateral MRP3 and MRP4 transporters export conjugated BAs from the hepatocytes using ATP as a source of energy, but not only BAs are transported from the cells. For instance, MRP3 is associated with resistance to methotrexate by pumping this drug out of the treated cells (Kool et al. 1999).

Organic solute transporters

Another type of transporters relevant mainly to BA efflux into the blood, especially under the cholestatic conditions, is the **organic solute and steroid transporter OSTα-OSTβ** (Ballatori et al. 2010, Boyer et al. 2006). However, the transport was demonstrated to be in both directions via facilitated diffusion. Whether uptake or efflux occurs, it depends on the electrochemical gradient (Ballatori et al. 2005).

This heteromeric complex transporter is located at the basolateral membranes of epithelial cells; the most important cells worth mentioning are hepatocytes, cholangiocytes and enterocytes. On the list of substrates typical for OSTα-OSTβ are BAs and conjugated steroids such as endogenous cholesterol metabolites or steroid hormones (Ballatori et al. 2010).

3.4.2 Hepatobiliary canalicular transporters

The canalicular transporters are crucial for BA secretion from hepatocytes into the bile canaliculi. There are several crucial transporters dependent on ATP and belonging to the **ABC transporters** (Dawson et al. 2009).

Bile salt export pump

The principal transporter for efflux of conjugated BAs into the bile canaliculi is the **bile salt export pump** with the human gene name **ABCB11**. The location of this transporter is at the canalicular (apical) membrane of hepatocytes. This transporter works on the basis of active transport due to the fact that the concentration of BAs in bile is much higher than within the hepatocytes (Dawson et al. 2009).

Multidrug resistance proteins and cholesterol transporters

Another ABC family member is the **multidrug resistance protein 3 (MDR3)**. The MDR3 transporter is encoded by the gene **ABCB4**. This transporter mediates transport of phospholipids into the bile. No less important, the two members of ABC subfamily G, namely **ABCG5** and **ABCG8,** are involved in cholesterol efflux into the bile (Graf et al. 2003, Morita and Terada 2014).

Multidrug resistance-associated proteins

The member of the **multidrug resistance-associated proteins** located in hepatocytes at the canalicular membrane is **MRP2** encoded by the gene **ABCC2**. The main substrates transported by MRP2 into the canaliculi are conjugates with glutathione and glucuronic acid or other anionic compounds (König et al. 1999).

As the name of this family of transporters suggests, these proteins cause resistance to certain drugs (cytostatics mainly) by transporting the drug's conjugates out of the cells (Kool et al. 1999, König et al. 1999).

4 AIMS OF THE THESIS

The aim of presented thesis is to investigate the molecular mechanisms of AMO/CLA DILI in two *in vitro* human hepatocellular models: HepG2 and Upcyte hepatocytes. Most of the published clinical reports classify AMO/CLA DILI as cholestatic (deLemos et al. 2016, Lucena et al. 2006, Robles et al. 2010), but the pathogenesis of this hepatotoxicity at the molecular level is still not completely known.

First, the determination of cytotoxic concentrations of AMO and AMO/CLA on the model hepatocyte systems, HepG2 and Upcyte, will be evaluated using a cell viability test (MTT assay). For subsequent experiments, only non-cytotoxic concentrations will be used to avoid mixed side effects triggered by the activation of necrotic and apoptotic pathways at cytotoxic concentrations.

After treatment with the studied hepatotoxic drugs, the gene expression levels of key hepatobiliary transporter, enzyme and NR messenger RNAs (mRNAs) will be evaluated using quantitative real-time polymerase chain reaction (q-RT-PCR). The attention will be paid to the levels of the basolateral transporters NTCP, MRP3, MRP4, OSTα and OSTβ; the canalicular transporters BSEP, MRP2, MDR3, ABCG5 and ABCG8; enzymes CYP7A1, CYP8B1, CYP27A1, HMGCR, UGT2B4 and NRs SHP and LXR. For this purpose, methods of RNA extraction, electrophoresis on an agarose gel and reverse transcription will be needed.

As Upcyte cells show a preserved phenotype expressing more important hepatobiliary transporters than HepG2 cells (Tolosa et al. 2016), human Upcyte hepatocytes will be used for the Western blot analysis of two crucial protein transporters, BSEP and NTCP, thus protein extraction and quantification will be necessary.

In addition, the image documentation of HepG2 and Upcyte hepatocytes treated with AMO, AMO/CLA and VALP or with combinations of these drugs and selected BAs will be presented using images from an inverted light microscope.

5 EXPERIMENTAL PART

5.1 Materials and reagents

5.1.1 List of chemicals

- Acrylamide 40 % – Anresco
- Agarose D1 low EEO – Laboratorios Conda
- Ammonium persulphate (APS) 10 % – Bio-Rad
- Amoxicillin – Sigma Aldrich
- Amoxicillin trihydrate / potassium clavulanate (4:1) – Sigma Aldrich
- β-Mercaptoethanol – Merck
- Bovine serum albumine (BSA) – Gibco
- Collagen from rat tail tendon – Roche
- Dimethyl sulfoxide (DMSO) – Fagron
- DNA gel loading buffer 6× – Fagron
- Deoxy-nucleotides (dNTP's) – Invitrogen
- Dried milk – Austriana
- Dithiothreitol (DTT) – Invitrogen
- Ethanol 20 % – PanReac AppliChem Reagents
- Ethylenediaminetetraacetic acid (EDTA) 0.5 M – Thermo Fisher Scientific
- Fetal bovine serum – Thermo Fisher Scientific
- First-Strand buffer 5× – Invitrogen
- GeneRuler 100 bp – Thermo Fisher Scientific
- Glycine – Sigma Aldrich
- Haet™ protease & phosphatase inhibitor cocktail – Thermo Fisher Scientific
- Ham's F-12 medium – Gibco
- Laemmli sample buffer 4× – Bio-Rad
- Leibovitz's L-15 medium – Gibco
- Light Cycler® FastStar DNA master SYBR Green I – Roche
- L-Glutamine – Merck
- Methanol – Merck
- Moloney-Murine Leukemia Virus (M-MLV) reverse transcriptase – Invitrogen
- M-PER® Mammalian protein extraction reagent – Thermo Fisher Scientific

- Methylthiazolyldiphenyl tetrazolium bromide (MTT) – Sigma Aldrich
- Oligo-deoxy-thymidine (oligo dT14)– Invitrogen
- Penicillin – Sigma Aldrich
- Phosphate-buffered saline (PBS) – Thermo Fisher Scientific
- Potassium chloride (KCl) – Merck
- Precision Plus Protein™ dual colour standard ladder – Bio-Rad
- Quinoline yellow – Sigma Aldrich
- RNaseOut recombinant ribonuclease inhibitor – Invitrogen
- Sodium bicarbonate ($NaHCO_3$) – Sigma Aldrich
- Sodium chloride (NaCl) – Carlo Erba Reagents
- Sodium dodecyl sulphate (SDS) – Merck
- Sodium valproate – Sigma Aldrich
- Specific primers – Invitrogen
- Streptomycin – Sigma Aldrich
- SYBR® Safe DNA Gel Stain – Thermo Fisher Scientific
- SYBR® Green DNA I Master – Roche
- Tetramethylethylenediamine (TEMED) – Bio-Rad
- Tris(hydroxymethyl)aminomethane (Tris) – Sigma Aldrich
- Trypan Blue Dye – Carlo Erba Reagents
- Trypsin – Thermo Fisher Scientific
- Tween-20 – Merck
- Upcyte® High Performance Medium – Upcyte® technologies GmbH
- Upcyte® Supplement A – Upcyte® technologies GmbH
- Upcyte® Supplement B – Upcyte® technologies GmbH
- Xylene cyanole blue dye – Sigma Aldrich

5.1.2 List of commercial kits

- Bradford Protein Assay Kit – Bio-Rad
- Clarity™ Max Western ECL Substrate Kit – Bio-Rad
- Clarity™ Western ECL Substrate Kit – Bio-Rad
- RNeasy® Mini Kit 250 – Qiagen
- Trans-Blot® Turbo RTA Transfer Kit – Bio-Rad

5.1.3 List of specific primers

All specific primers used for quantitative real-time polymerase chain reaction experiments were purchased from Invitrogen™ (Thermo Fisher Scientific) and their sequences are listed below.

Genes of interest

• ABCG5	Forward:	ATGGAAGTGAAGCTGCCGACT
	Reverse:	TTACATTCTTGGGTCCGCTCA
• ABCG8	Forward:	GTGTCCTTCCTGCGGTGGT
	Reverse:	GACGATGAGGTAGATGGCGTAG
• BSEP	Forward:	GGGCTCCATTTCAGCTATGT
	Reverse:	ACTTGCGAGTCAGGTCGAG
• CYP27A1	Forward:	ATGGCTGGAGTGGACACGAC
	Reverse:	ACCACAGGGTAGAGACGCAG
• CYP7A1	Forward:	GCATGCTGTTGTCTATGGCTT
	Reverse:	AACTCAAGAGGATTGGCACCA
• CYP8B1	Forward:	TGGACCCTGACACACCACTA
	Reverse:	GGCCAAGCTCACTCTGTAGG
• HMGCR	Forward:	AAGCCTGTTTGCAGATGCTAGG
	Reverse:	GCCATTACGGTCCCACACAC
• LXR	Forward:	AAGCGGCAAGAGGAGGAACAG
	Reverse:	GCTCAGTGAAGTGGGCAAAGC
• MDR3	Forward:	GAAGAAAGGCCAGACACTAGC
	Reverse:	CTGAGACACGATTCCGAGTT
• MRP2	Forward:	GCCGGTGGTCAGATTATCAT
	Reverse:	GATCTTGGATTTCCGAAGCA
• MRP3	Forward:	TGAGATCCTGAACGGCATCAAG
	Reverse:	GCACATTGTTTGGGTCCACGTA
• MRP4	Forward:	ATTTATCGGAAGGCACTTCGT
	Reverse:	CAAGGGCAGGAGAATGATTAGA
• NTCP	Forward:	CTGCTGGGTTATGTTCTCTCTGC
	Reverse:	CCAATGACTTCAGGTGGAAAGGC
• OSTα	Forward:	TGGGCATCATTTCCCGTCAAG
	Reverse:	GTAGGGCAGTCAGGATGAGGA

- OSTβ Forward: ATCCAGGCAAGCAGAAAAGA
  Reverse: CTGGTACATCCGGAAGGAAA
- SHP Forward: CAGCAGCAGTGGAGGCAGTG
  Reverse: CGGGGTTGAAGAGGATGGTC
- UGT2B4 Forward: CACAGAATTCAGCCACTGGA
  Reverse: CTGCCCATCTCTTAACCAGC

Reference genes

- ACTβ Forward: CGTACCACTGGCATCGTGAT
  Reverse: GTGTTGGCGTACAGGTCTTTG
- PBGD Forward: CGGAAGAAAACAGCCCAAAGA
  Reverse: TGAAGCCAGGAGGAAGCACAGT

5.1.4 List of antibodies

Primary antibodies for Western blot

- Anti-BSEP (F6), mouse monoclonal antibody, dilution: 1:500, AB71793 – Santa Cruz Biotechnology, Inc.
- Anti-NTCP, rabbit polyclonal antibody, dilution: 1:1000, AB131084 – Abcam
- Anti-GAPDH (G9), mouse monoclonal antibody, dilution: 1:500, sc-365062 – Santa Cruz Biotechnology, Inc.

Secondary antibodies for Western blot

- Anti-Mouse, goat polyclonal imunoglobulines, dilution: 1:1000, P0447 – Dako Denmark
- Anti-Rabbit, goat polyclonal imunoglubulines, dilution: 1:2000, P0448 – Dako Denmark

5.1.5 List of equipment and disposable tools

- Automatic pipettes – Gilson and Eppendorf
- Automatic multichannel pipettes – Gilson and Eppendorf
- Cell culture 6-, 12-, 24- and 96-well plates – Thermo Fisher Scientific

- Cell culture 12-, 24- and 96-well plate with collagen coating – BioCoat, Corning
- Cell culture flasks – Thermo Fisher Scientific
- Cell culture flasks with collagen coating – BioCoat, Corning
- Cellulose acetate filters, sterile, 0.2 μm – Sartorius Stedim Biotech
- Electronic single channel pipettes – Gilson
- Electrophoresis buffer tank and lid – Bio-Rad
- Hemocytometer – Abcam
- Microcentrifuge tubes – Eppendorf
- Parafilm – Ted Pella, Inc.
- Pipet tips 0.5 μL – 5000 μL – Thermo Fisher Scientific
- Syringes, sterile, 3, 5, 10 mL – Sigma Aldrich
- 384-well plates for q-RT-PCR – Roche

5.2 Devices and software

5.2.1 List of devices

- Amersham Imager 600 – GE Healthcare Life Sciences
- Analytical balance Gram precision series ST – Gram group
- Analytical balance Cobos precision CB – Cobos
- Autoclave – Trade Raypa
- Cell culture Incubator Certomat® H – B-Braun
- Cell culture Incubator HERAcell® – Heraeus
- Centrifuge 5417R – Eppendorf
- Centrifuge Heraeus Megafuge 40R – Thermo Fisher Scientific
- Centrifuge for plates Scan Speed 1236R – Labogene
- Electrophoresis power supply Apelex PS 304 minipac II – Analytic Jena
- Electrophoresis power supply PowerPac™ basic – Bio-Rad
- Gel Logic 200 Imaging System and Camera – Kodak
- Laminar airflow cabinet Faster Two 30 – Mason Technology
- Laminar airflow cabinet HERAcell® – Heraeus
- Light Cycler® 480 – Roche
- Magnetic shaker Selecta P – Agimatic-S

- Microscope DMI 4000 B – Leica
- Microwave oven Microondas FM 1335 – Daewoo
- Spectrophotometer NanoDrop 2000 – Thermo Fisher Scientific
- Spectrophotometer Plates Reader Halo Led 96 – Dynamica
- Thermoblock & Thermomixer comfort and compact – Eppendorf
- Trans-Blot® Turbo™ Transfer System – Bio-Rad
- UV Transilluminator Gel Logic 2000 – Kodak
- Vortex Genie 2 – Scientific industries
- Water Baths – Ovan

5.2.2 List of software

- Amersham Imager 600 software – GE Healthcare Life Sciences
- Capture 96 software – Dynamica
- ChemDraw Professional – Perkin Elmer
- Gel Logic 200 Imaging System – Kodak
- GraphPad Prism 7 – GraphPad software
- LightCycler Relative Quantification Analysis software – Roche
- Microsoft Office – Microsoft Corporation
- NanoDrop 2000 software – Thermo Fisher Scientific

5.3 Methods

5.3.1 Hepatocyte cell lines and cultures

Two different types of human hepatocytes were used for the experiments about AMO or AMO/CLA hepatotoxicity. The first set of experiments was performed with **HepG2 cell line**. The second set of experiments was performed with human **Upcyte hepatocytes**. Each type of hepatocyte-derived cell has its own advantages and disadvantages, which are briefly described below.

HepG2 cell line

HepG2 cells (ATCC HB-8065, Rockville, Maryland, USA) are human liver adherent and epithelial-like cells derived from a hepatocellular carcinoma from a 15-year-old Caucasian American male. This cell line was used due to its common and widespread application in different hepatological studies and usage as a cell model for hepatotoxicity assessment. Another advantage of HepG2 is the simple way of handling during culturing and treatment (Fernández-Murga et al. 2018).

The problematic side of using HepG2 consists in the poor expression of some important metabolic enzymes, especially enzymes typical for phase I drug metabolism (for example cytochromes P450), but also specific BA transporters (for example BSEP or NTCP) (Wilkening et al. 2003, Donato et al. 2013).

HepG2 cells were cultured in **HepG2 Full Medium** with the composition listed in Table 2. Cells were maintained at 37 °C and 5 % CO_2 in 95 % humidified atmosphere. Medium was changed every 3 days of culturing, and if needed (when the confluence of cells reached 70-80 %), passaging of cells was performed by firstly washing with PBS and secondly with 0.25 % trypsin / 0.02 % EDTA preheated at 37 °C. Detached HepG2 cells were collected and seeded in new flasks or x-well plates.

Table 2 ***The composition of HepG2 Full Medium***

Components		Final concentration
Glucose (5 mM)	500 μL	25 μM
L-Glutamine (200 mM)	1 mL	2 mM
Penicillin-Streptomycin (5 000 Units/mL of Penicillin 5 000 μg/mL of Streptomycin)	1 mL	50 Units/mL of Penicillin 50 μg/mL of Streptomycin
Sodium bicarbonate – $NaHCO_3$ (1 M)	1.2 mL	12 mM
Bovine serum albumin – BSA (100 mg/mL)	2 mL	2 mg/mL
Fetal bovine serum	7 mL	7 %
Ham's F12 Medium	45 mL	-
Leibovitz's L15 Medium	45 mL	-

For cell viability assay (MTT assay), HepG2 cells were seeded in 96-well plates (1.5×10^4 cells / well) with HepG2 Full Medium and were allowed to grow until the confluence reached about 70 % (approximately one day). The medium was removed when the desired confluence was reached, and treating solutions in a final volume of 100 μL / well were incorporated. The treatments lasted for 24 hours.

For gene expression experiments, HepG2 cells were cultured in 12-well plates (3.0×10^5 cells / well) or 24-well plates (1.5×10^5 cells / well) with HepG2 Full Medium and were allowed to grow until the confluence reached about 70 % (approximately one day). Medium was removed when the desired confluence was obtained, and treating solutions were applied in a volume of 1 mL or 500 µL / well, respectively. The treatments lasted for 24 hours.

Upcyte hepatocyte cell cultures

The second model type of hepatocytes used in this work are the Upcyte expanded primary hepatocytes. The Upcyte® technology is a novel technique able to force primary human hepatocytes to proliferate several times and concurrently conserve some specific functions. They have been derived from several donors and preserve a similar phenotype to that of primary cultured hepatocytes (Tolosa et al. 2016). The human Upcyte® hepatocytes donors used for the experiments in this thesis were obtained from Ucpyte® technologies GmbH (Hamburg, Germany) and are coded as 10-03 (48-year-old) and 422A-03 (neonate).

Upcyte cells were seeded in collagen type-I pre-coated flasks and 6-, 12-, 24- and 96-well plates. Upcyte hepatocytes were cultured either on a collagen monolayer or in a double-collagen sandwich configuration. The **Upcyte Expansion Medium** was used with the composition listed in Table 3. The incubation conditions were maintained at 37 °C and 5 % CO_2 in 95 % humidified atmosphere. The medium was changed every 2 days of culture, and if needed (when the confluence of cells reached 70-80 %), cells were detached by firstly washing with PBS, followed by detaching with 0.25 % trypsin / 0.02 % EDTA preheated at 37 °C and seeding at the density of 5 000 cells / cm^2 in new flasks.

Table 3 ***The composition of Upcyte Expansion Medium***

Components		Final concentration
Upcyte® Hepatocyte High Performance Medium	500 mL	-
Upcyte® Supplement A	5 mL	-
Upcyte® Supplement B	50 µL	-
L-Glutamine	5 mL	-
Penicillin-Streptomycin (5 000 Units/mL of Penicillin 5 000 µg/mL of Streptomycin)	5 mL	50 Units/mL of Penicillin 50 µg/mL of Streptomycin

For cell viability assay (MTT assay), Upcyte cells were seeded in collagen type-I pre-coated 96-well plates (1.5×10^4 cells / well) with Upcyte Expansion Medium and were allowed to grow until the confluence reached about 70-80 %. Subsequently, medium was removed when the desired confluence was reached, and treating solutions in a volume of 100 µL / well were incorporated. After 24 hours of treatment, the MTT assay was performed.

For gene expression experiments, Upcyte cells were seeded in collagen type-I pre-coated 12-well (3.0×10^5 cells / well) or 24-well plates (1.5×10^5 cells / well) with Upcyte Expansion Medium. When cells were 100% confluent (4 to 6 hours later), medium was replaced with **Upcyte Maintenance Medium** (i.e. Upcyte Expansion Medium without Supplement B). On the next day (Day 0), plates were placed on ice, Upcyte Maintenance Medium was removed and a second layer of neutralized collagen from rat tail tendon, prepared according to the manufacturer's instructions, was applied over the cells and allowed to polymerize for 1 hour in the cell culture incubator. Then, Upcyte Maintenance Medium was added again to each well. During this step, plates were put on ice until medium was added to all wells to prevent drying. The medium was changed every 2 days of culture (Day 2 and Day 4). Subsequently (Day 5), when Upcyte hepatocytes reach to the maximum expression of several key transporters and enzymes (Petrov et al. 2018), medium was removed and treating solutions in a final volume of 1 mL or 500 µL / well were incorporated, respectively. The treatments lasted for 24 hours.

For protein extraction, the same procedure (Figure 5) was repeated with Upcyte cells seeded in a double-collagen sandwich format in 6-well plates using 2 mL of treating solutions / well. The treatments lasted for 24 and 48 hours.

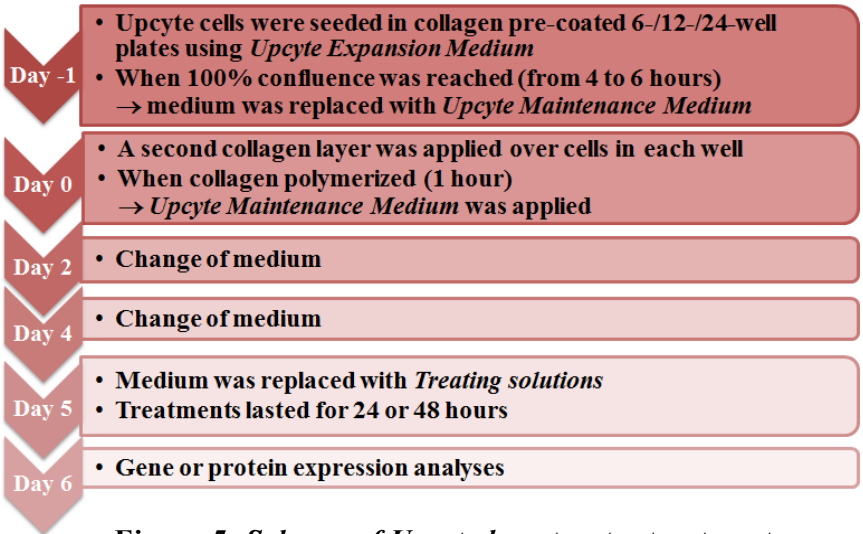

Figure 5 ***Scheme of Upcyte hepatocytes treatment***

5.3.2 Treatment with studied compounds

The solutions of studied compounds, **amoxicillin** and **amoxicillin trihydrate / potassium clavulanate**, were prepared directly in cell medium (HepG2 Full Medium or Upcyte Maintenance Medium**)** immediately before treatment. The compounds were weighed, dissolved in cell medium preheated at 37 °C and the solutions were filtered with a cellulose acetate sterile filter of 0.2 μm pore size before adding to cells.

Valproic acid was chosen as a model steatotic / cholestatic drug. The stock solution of **sodium valproate** was prepared in dimethyl sulfoxide (DMSO) and subsequently mixed with cell medium to obtain the required concentration of 4 mM just before treatment (Donato et al. 2016, Tolosa et al. 2018).

The used concentrations of VALP, AMO and CLA for HepG2 cells were chosen according to reviewing literature (De Abrew et al. 2016, Tolosa et al. 2018). On the other hand, there have not been reported any previous studies about VALP, AMO and CLA for Upcyte cells. Therefore, the cell viability assay (MTT assay) was performed first in order to exclude cytotoxic concentrations. The treating solutions with concentrations of AMO 0.02, 0.1, 0.5, 2.5, 5, 10 and 20 mM and AMO/CLA 0.02/0.01, 0.1/0.04, 0.5/0.2, 2.5/1.1, 5/2.2, 10/4.4 and 20/8.9 mM in cell medium were prepared for MTT assays performed in HepG2 and Upcyte cells. For further set of experiments, only non-cytotoxic concentrations for each hepatocellular model were chosen separately. The selected concentration of VALP (4 mM) was used as a concentration able to cause significant changes in gene expression levels according to previous study in rat hepatocytes (Donato et al. 2016).

HepG2 and Upcyte cells were treated for 24 or 48 hours and after this period, medium was removed, cells were washed with PBS and plates were frozen at -80 °C until the RNA or protein extractions were performed.

To imitate cholestatic conditions in hepatocytes, HepG2 cells were treated with a 160 μM **mixture of BAs** containing 12 most common BA species (Petrov et al. 2018). The relative concentration of each BA in this pool reproduced the relative concentration in human serum (Table 4).

Table 4 ***The mixture of BAs with relative concentrations of each BA***

Relative concentration	Used bile salt	Bile acid
9.3 %	Na^+ Cholate	Cholic acid
9.6 %	Na^+ Glycocholate	Glycocholic acid
1.2 %	Na^+ Taurocholate	Taurocholic acid
13.0 %	Na^+ Chenodeoxycholate	Chenodeoxycholic acid
36.8 %	Na^+ Glycochenodeoxycholate	Glycochenodeoxycholic acid
5.5 %	Na^+ Taurochenodeoxycholate	Taurochenodeoxycholic acid
12.6 %	Na^+ Deoxycholate	Deoxycholic acid
8.6 %	Na^+ Glycodeoxycholate	Glycodeoxycholic acid
1.5 %	Na^+ Taurodeoxycholate	Taurodeoxycholic acid
0.6 %	Na^+ Lithocholate	Lithocholic acid
1.0 %	Na^+ Glycolithocholate	Glycolithocholic acid
0.3 %	Na^+ Taurolithocholate	Taurolithocholic acid

5.3.3 Counting of viable cells

The number of viable cells in cell suspension was calculated using hemocytometer and Trypan blue dye. In the first step, 50 μL of cell suspension were mixed with 50 μL of Trypan blue. In the second step, 100 μL of new suspension were pipetted into the hemocytometer. Viable cells, which remained unstained, were counted using a microscope (10× magnification) and the quantity of live cells was calculated using standard formula:

$$\frac{a+b+c+d}{4} \times DF \times 10\,000 = Viable\ cells/mL$$

Explanatory notes: a, b, c, d stand for a number of cells in one set of 16 squares (1 mm^2), *DF* means dilution factor (cell suspension after Trypan blue addition), 10 000 is correction factor for volume.

5.3.4 Cell viability assay

The MTT cell viability assay is a method for obtaining information about cell viability and estimating approximate percentage of viable cells among all treated cells. According to this method, cytotoxicity of specific compounds can be estimated. The method is terminal and therefore cells cannot be used again, because the reagent penetrates across membranes of viable cells and the product of the reaction destroys viable cells in the end (Mosmann 1983, Sittampalam et al. 2004).

The principle is based on the ability of viable cells to transform a yellow coloured MTT [3-(4,5-dimethylthiazol-2-yl)-2,5-diphenyltetrazolium bromide] into a visibly purple product called formazan, which can be measured spectrophotometrically with the maximum absorbance near 570 nm. The transformation of MTT into formazan is done by active mitochondrial metabolism. If the cells are dead, there will be no active metabolism and no production of purple formazan. This means: the higher absorbance, the higher the number of living cells (Mosmann 1983, Sittampalam et al. 2004).

Design of the MTT assay was adjusted for 96-well plates (Figure 6) with HepG2 or Upcyte cells. Spectrophotometer plate reader Dynamica and Software Capture 96 were used for the measuring of absorbance.

1. Firstly, the mixture of MTT and cell medium has to be prepared. For each 10 mL of medium, 1 mL of MTT was used and this working solution was stored with protection against direct light.
2. After 24 hours of treatment with treating solutions, medium was removed from each well of 96-well plate and adherent cells at the bottom of each well were washed with 100 μL of PBS preheated at 37 °C. After that, PBS was removed.
3. To each well, 100 μL of MTT working solution were added and plate was incubated for 2 hours at 37 °C in the dark settings of an incubator.
4. After the incubation period, MTT working solution was removed and each well was washed with 100 μL of PBS.
5. For dissolving the generated formazan, 100 μL of DMSO were used for each well and after 10 minutes of incubation at room temperature following with 5 seconds of shaking, the absorbance was measured at 550 nm.
6. Results were processed using Excel-Office software. Graphs were made using GraphPad Prism 7 software.

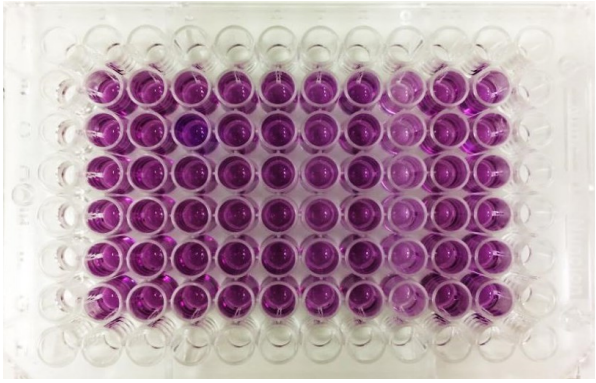

Figure 6 ***A 96-well plate of HepG2 cells after MTT assay***

5.3.5 RNA extraction

The process of RNA extraction was carried out according to the protocol of commercial **RNeasy® Mini Kit 250** (Qiagen) and was slightly modified in several steps. The exact procedure with small changes is thoroughly described below.

The RNeasy® Mini Kit 250 was generally designed for the extraction and purification of total RNA from cells, tissues or yeasts by using the silica-membrane RNeasy® Mini Spin Columns. The binding capacity of these commercial columns was stated to be 100 μg of RNA. All reagents needed were included in the mentioned kit. The purity and concentration of extracted RNA was measured on Spectrophotometer NanoDrop 2000. The measuring of optical density (OD) at 260 nm was used for quantification and calculation of OD_{260}/OD_{280} ratio was used for purity determination. As a blank, RNase-free water was used, the same as was used for RNA extraction.

1. After 24 hours of treatment with treating solutions, cells were frozen (-80 °C) in original 12- or 24-well plates without medium until the RNA extraction was performed. For the first step, 350 μL of Lysis Buffer RLT with 1 % of β-Mercaptoethanol were added to each well and cells were scraped with sterile syringes without needles. After this step of detaching, the syringes with needles were used to collect and transfer samples into sterile microcentrifuge tubes.
2. Then, 350 μL of Ethanol 70 % were added to each lysate. Everything was mixed properly by pipetting until the turbidity in lysates disappeared.
3. All samples, each with a total volume of 700 μL, were transferred to the RNeasy® Mini Spin Columns, which were placed in 2 mL collecting tubes. The centrifugation for 15 seconds at 10 000 ×G at 21 °C was followed and the flow-through was discarded.
4. In the next step, 700 μL of Buffer RW1 were added to each column and centrifuged for 15 seconds at 10 000 ×G at 21 °C. The flow-through was discarded.
5. Into each column, 500 μL of Buffer RPE were added and centrifuged for 15 seconds at 10 000 ×G at 21 °C. The flow-through was discarded.
6. Previous step was repeated by adding 500 μL of Buffer RPE, but columns were centrifuged for 2 minutes at 10 000 ×G at 21 °C. The flow-through was discarded and the RNeasy® Mini Spin Columns were placed into new 2 mL collection tubes. Everything was centrifuged again for 1 minute at high speed of 20 000 ×G at 21 °C.

7. The columns were relocated in new 1.5 mL microcentrifuge tubes intended for storage of the extracted RNA. The lids of all columns were opened at once and let for 5 minutes to evaporate ethanol contained in the used buffers.
8. To each column, 45 μL of RNase-free water were added directly onto the column membrane and everything was centrifuged for 1 minute at 10 000 ×G at 4 °C to elute the RNA from the membrane. Once RNA was obtained, the microcentrifuge tubes were placed on ice immediately and measuring of OD followed.

5.3.6 Electrophoresis on agarose gel

The integrity and purity of extracted RNA was affirmed by running 1 % agarose gels in Tris-Acetate-EDTA buffer (TAE buffer) on horizontal electrophoresis. For preparing gels, 1 g of Agarose D1 Low EEO was boiled in 100 ml of TAE buffer and 10 μL of SYBR® Safe DNA Gel Stain 10 000× were added when the temperature of dissolved agarose reached approximately 60 °C and poured into the cassette immediately. After at least 30 minutes of solidifying, the samples were loaded on wells and electrophoresis was carried out with voltage of 80 Volts for 40 minutes.

Each loaded sample (10 μL) contained 5 μL of diluted RNA to obtain equal concentration (90-100 ng/μL), 5 μL of RNase-free water and 2 μL of Loading Buffer 6× (total volume of 12 μL). GeneRuler 100 bp was used as a ladder.

The gel with bands stained with SYBR® Safe DNA Gel Stain was viewed using the UV Transilluminator Gel Logic 200 and images were captured with built-in camera and software from Kodak Company (Figure 7).

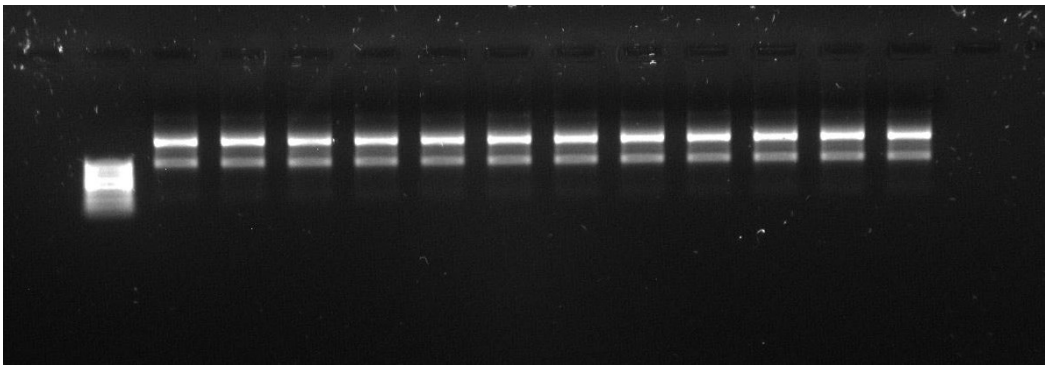

Figure 7 ***The samples of extracted RNA after running the agarose electrophoresis***

5.3.7 Reverse transcription

After obtaining total RNA from hepatocytes, reverse transcription was followed. The reaction of reverse transcription is characterized by transcription of RNA template into the complementary DNA (cDNA) by using the enzyme of reverse transcription (Degen et al. 2006).

For the experiments of this thesis the following reagents were used: M-MLV reverse transcriptase 200 U, deoxy-nucleotides (dNTPs), oligo-deoxy-thymidine primers (oligo dT), First-Strand buffer 5×, 0.1 M dithiothreitol (DTT) and RNase inhibitor. For each reaction of reverse transcription, 10 μL of diluted RNA (90-100 ng/μL) were mixed with 20 μL of reagent mixture to create initial sample. For each set of reverse transcription reactions a blank was prepared.

1. The first step was characterized by putting samples on water bath preheated at 42 °C for 60 minutes. During this phase, reverse transcriptase is working to create new complementary strand of DNA.
2. In the second step, the function of reverse transcriptase is stopped by placing the samples in a thermoblock preheated at 70 °C for 15 minutes. After that, the samples were placed on ice, centrifuged and diluted to obtain concentration of 1.1 ng / μL.

5.3.8 Quantitative real-time polymerase chain reaction

The general principle of polymerase chain reaction is to amplified particular sequences of DNA or cDNA template. For this reaction, specific forward and reverse primers, nucleotides, thermo-stable DNA-polymerase and thermal cycler are needed. The main advantage of quantitative real-time polymerase chain reaction (q-RT-PCR) is that the product of reaction, amplicon, is quantified after each cycle and the initial concentrations of studied sequences of cDNA can be determined with relatively high precision. The quantification is carried out on the basis of a fluorescent signal of SYBR Green dye incorporated into double-stranded DNA (Degen et al. 2006).

Firstly, the initial samples of cDNA were diluted to the concentration about 1.1 ng / μL as an effective amount for q-RT-PCR (Degen et al. 2006). Described yellow-coloured solution was used for diluting cDNA: 1 000 μL Tris-EDTA buffer 1× (TE buffer) + 100 μL quinoline yellow 200× + 8 900 μL distilled and deionized water

(DDI H_2O). The obtained concentrations were confirmed on Spectrophotometer NanoDrop 2000 by measuring OD at 260 nm.

After preparation of necessary reagents, 2.5 µL of diluted cDNA were mixed together with 7 µL of blue-coloured mastermix reagents for q-RT-PCR (1.72 µL DDI H_2O + 3.6 µL SYBR® Green DNA I Master + 0.08 µL xylene cyanole + 0.8 µL diluted forward primer + 0.8 µL diluted reverse primer / per one reaction) in the microwells of 384-well plates for q-RT-PCR and processed in thermal cycler LightCycler® 480 Roche. The list of all specific primers is summarized in the chapter 5.1.3 (List of specific primers).

In parallel with the studied genes of several key BA transporters, enzymes and NRs, human housekeeping genes for β-Actin (ACTβ) and Porphobilinogen deaminase (PBGD) were analyzed and their mRNA levels were used as an internal normalization reference for HepG2 and Upcyte cells, respectively.

The PCR cycling conditions consisted in the initial denaturation (95 °C, 8 minutes); followed by the cycles of denaturation (95 °C, 15 seconds), annealing (59 °C, 20 seconds) and extension (72 °C, 30 seconds), for a total number of 40 cycles; followed by final extension (72 °C, 10 minutes). The LightCycler Relative Quantification Analysis software was used for real-time monitoring and product quantification in the exponential phase of the amplification. Results were processed using Excel-Office software and are expressed as fold-change to the mRNA level observed in control samples. Graphs and statistical analysis were made using GraphPad Prism 7 software.

5.3.9 Protein extraction

1. For obtaining total protein from cells, medium was gently removed, cells were washed with ice-cold PBS and, if needed, the 6-well plate was frozen at -80 °C until the protein extraction was processed.
2. If freezing was necessary, the plate was put on ice to be slowly thawed. Thereafter, 200 µL of protein extraction solution with the composition listed in Table 5 were added into each well of 6-well plate, followed by incubation on ice for 20 minutes with slow agitation.

Table 5 ***Reagents used for protein extraction***

Components	Volume
M-PER® Mammalian protein extraction reagent	1000 μL
Heat™ Protease & Phosphatase inhibitor cocktail	10 μL
0.5 M EDTA solution	10 μL

3. The lysated samples were collected into microcentrifuge tubes and centrifuged at 14 000 ×G for 20 minutes at 4 °C.
4. After centrifugation, the supernatants containing total protein were transferred into new microcentrifuge tubes and kept in the freezer at -80 °C until next step.

5.3.10 Protein quantification

The quantification of total protein extracted from cells was followed according to the manufacturer's instruction for the **Bradford Protein Assay Kit** (Bio-Rad). The principle of this colorimetric method is based on the ability of Coomassie brilliant blue dye to bind proteins while its colour changes from red (protonated form) to blue (unprotonated form). When the dye is in neutral conditions, the green colour predominates (Bradford 1976). The protein concentration was indirectly measured spectrophotometrically with a plate reader Spectrophotometer Dynamica as an absorbance of blue-coloured product at a wavelength of 550 nm.

Regarding methods of protein quantification, it is important to have on mind that AMO interferes with commonly used protein quantification procedures. The Biuret, Lowry and Bicinchoninic acid methods are needed to be excluded as AMO reacts with used reagents and then method gives changed values (Williams et al. 2003).

1. Firstly, the protein standard (bovine serum albumin) dilutions were prepared to obtain calibration curve. Secondly, the diluted dye reagent was prepared by mixing 1 part of Coomassie brilliant blue dye concentrate from the commercial kit and 4 parts of DDI H_2O.
2. The procedure of quantification was performed in 96-well plates (Figure 8). Each well contained 10 μL of protein standard or sample, and 200 μL of diluted dye reagent. All samples and standards were prepared as triplicates.
3. After pipetting all components and shaking for 30 seconds, incubation at room temperature for 5 minutes was done.

4. The absorbance was measured at 550 nm on a plate reader Spectrophotometer Dynamica. The protein concentration of each sample was determined using the calibration curve of the protein standard in Excel-Office software.

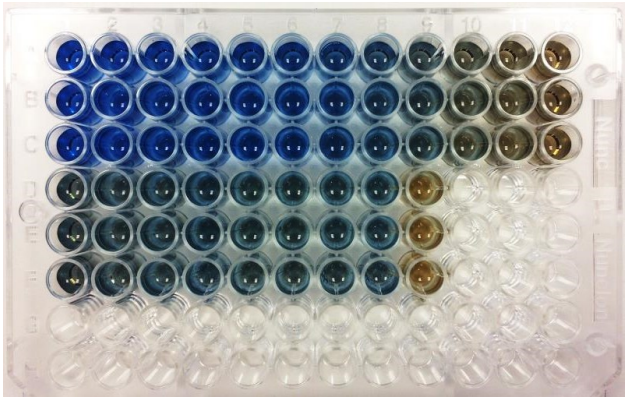

Figure 8 ***A 96-well plate of HepG2 after Bradford Protein Assay***

5.3.11 Western blot

The Western blot is a multistep method used for detection of specific proteins in the sample of total extracted proteins. In the first step, it is necessary to separate individual proteins. This separation is enabled with sodium dodecyl sulphate polyacrylamide gel electrophoresis (SDS-PAGE). Macromolecular proteins are sorted according to their weight and the diameter of the porous structure of the gel. After that, proteins are transferred to the membrane on which they can be labelled with specific antibodies (Mahmood and Yang 2012).

1. **Protein samples** – The samples for SDS-PAGE were obtained using the protein extraction method as was described previously. To load the same amount of proteins, it was necessary to quantify protein concentration and then mix samples with Laemmli sample buffer 4× (the formulation is seen in Table 6), then boil samples at 50 °C for 10 minutes (standardized for BSEP) or at 99 °C for 5 minutes (standardized for NTCP) and centrifuge at 16 000 ×G for 1 minute.

Table 6 ***The composition of Laemmli sample buffer 4x***

Components	Concentration
Tris-HCl (pH 6.8)	277.8 mM
Glycerol	44.4 % (v/v)
Lithium dodecyl sulphate	4.4 % (w/v)
Bromophenol blue	0.02 %
β-Mercaptoethanol	10 %

2. **SDS-PAGE** – For this kind of electrophoresis, two types of gels are required. The lower gel (resolving) is necessary for the separation and detection of proteins. The higher gel (stacking) is necessary for proper start of electrophoresis and forming of compact bands of proteins. The concentration of acrylamide in the resolving gel varies depending on the molecular weight of the protein to be detected (Mahmood and Yang 2012). For BSEP and NTCP separation, the concentration of 7.5 % and 12 % acrylamide was prepared, respectively. The compositions of stacking and resolving gels are seen in Table 7. All components were mixed together, but APS and TEMED were added under the hood protection as the last ones. Gels were prepared in Bio-Rad cassettes for mini gels (8.6 × 6.8 cm).

Table 7 ***The composition of stacking and resolving gels for SDS-PAGE***

	Stacking gel 4 % (5 mL)	**Resolving gel 7.5 % (10 mL)**	**Resolving gel 12 % (10 mL)**
0.5 M TrisHCl pH 6.8	1250 μL	-	-
1.5 M TrisHCl pH 8.8	-	2500 μL	2500 μL
DDI H_2O	3140 μL	5340 μL	3340 μL
40 % Acrylamide	530 μL	2000 μL	4000 μL
10 % SDS (v/v)	50 μL	100 μL	100 μL
20 % APS	25 μL	50 μL	50 μL
TEMED	5 μL	10 μL	10 μL

The samples, with equivalent amount of total protein (40 μg), were loaded on a gel placed in the Bio-Rad chamber filled with Running buffer (Table 8). Voltage of 100 V was set for the first 20 minutes to reach the line between stacking and resolving gel, and then voltage of 130 V was set for separation during about 1.5 hours for 2 gels in the Bio-Rad chamber. The Precision Plus Protein™ dual colour standard ladder was used to compare molecular weights of proteins and was loaded in a volume of 5 μL / well. The samples of human liver (healthy donors) from Biobank of cryopreserved livers (Hospital La Fe, Valencia, Spain), were used as positive controls for BSEP or NTCP visualization.

Table 8 ***The composition of Running buffer in distilled H_2O***

Components	**Concentration**
Tris	25 mM
Glycine	192 mM
SDS	0.1 % (v/v)

3. **Protein transfer** – The transfer of proteins from gel into the polyvinylidene difluoride (PVDF) membrane is the essence of Western blot analysis. All the reagents and membranes used were from the **Trans-Blot® Turbo RTA Transfer Kit** (Bio-Rad). First of all, PVDF membrane was activated by wetting in 100 % methanol for 20 seconds and then was immersed in Transfer buffer (Table 9) for 1 minute together with two transfer stacks of filter pads. The transferring sandwich of two transfer stacks, membrane and gel was placed into the Trans-Blot® Turbo Transfer Cassette (Bio-Rad) and processed in Trans-Blot® Turbo Transfer System (Bio-Rad) using constant electric current at 2.5 A and 25 V for 10 minutes.

Table 9 ***The composition of Transfer buffer in distilled H_2O***

Components	Concentration
Tris	10 mM
Ethanol	20 %
Glycine	100 mM

4. **Immunodetection with antibodies** – After the protein transfer, membrane was washed in Washing buffer (Table 10) for 5 minutes.

Table 10 ***The composition of Washing buffer – Tris-buffered saline and Tween (TBST)***

Components	Concentration
NaCl	130 mM
KCl	2.7 mM
Tris	24.8 mM
Tween-20	0.1 %

For protein detection is necessary to block the membrane with Blocking buffer (Table 11) for 1 hour at room temperature, followed by washing in TBST for 5 minutes and incubation with primary antibody overnight (18 hours) at 4 °C with continuous agitation. The primary antibodies were prepared in required concentrations in 5 % milk in TBST. After the first incubation, membrane was washed 4×10 minutes in TBST and then incubated with secondary antibody for 1 hour at room temperature with continuous agitation. The secondary antibodies were prepared in required concentrations in 0.5 % milk in TBST. After the second incubation, membrane was washed 4×10 minutes in TBST. Subsequently, membrane was incubated with chemiluminescent reagent Clarity™ Max Western

Substrate (Bio-Rad) for 5 minutes on a flat and clean surface. Bands of proteins were visualized using an image analyser Amersham Imager 600 GE Healthcare Life Sciences.

Table 11 ***The composition of Blocking buffer***

Components	Concentration
Dried milk	5 % (w/v)
Tris-Buffered Saline and Tween 0.1 % (TBST)	

5. **Stripping** – After the immunodetection, membrane was washed in TBST and stripped in Stripping buffer (Table 12) at 50 °C for 10 minutes. Subsequently, membrane was washed 5×10 minutes in TBST, blocked with Blocking buffer (Table 11) for 1 hour at room temperature and reprobed newly with different antibodies.

Table 12 ***The composition of Stripping buffer***

Components	Concentration
SDS	2 % (v/v)
TrisHCl pH 6.8	62.5 mM
β-Mercaptoethanol	0.8 %

5.4 Statistical analysis

The number of performed experiments is indicated in the legend under each figure. Results are expressed as mean ± SD. The values were analysed using Analysis of variance (ANOVA test) and Tukey's multiple comparisons test. Statistical comparisons and graphs were made using GraphPad Prism 7 software. Results are considered to be significant when p-value is $p < 0.05$ (*), $p < 0.01$ (*) and $p < 0.001$ (***).

6 RESULTS

6.1 Cell viability

The aim of the MTT assay was to define non-cytotoxic concentrations convenient for further experiments. An adequate number of viable cells is a necessary prerequisite for effective gene and protein expression, thus the cytotoxic concentrations need to be excluded. Furthermore, exclusion of cytotoxic concentrations prevents from developing mixed side effects triggered by the activation of necrotic and apoptotic pathways in the treated cells.

The viability of HepG2 and Upcyte hepatocytes from two donors (10-03 and 422A-03) was determined by the MTT assays. Cells were incubated for 24 hours with serially diluted concentrations of AMO (from 0.02 to 20 mM) or AMO/CLA (from 0.02/0.01 mM to 20/8.9 mM).

The results for HepG2 cells are shown in Figure 9 for AMO and Figure 10 for AMO/CLA. Regarding AMO, only the highest concentration (20 mM) showed a slight reduction of cell viability. Regarding AMO/CLA combinations, a slight reduction was seen even at lower concentrations (0.5/0.2 mM, 2.5/1.1 mM, 5/2.2 mM) and a very significant reduction (up to 60-20 %) was seen at the two highest concentrations (10/4.4 mM and 20/8.9 mM), therefore these concentrations were excluded.

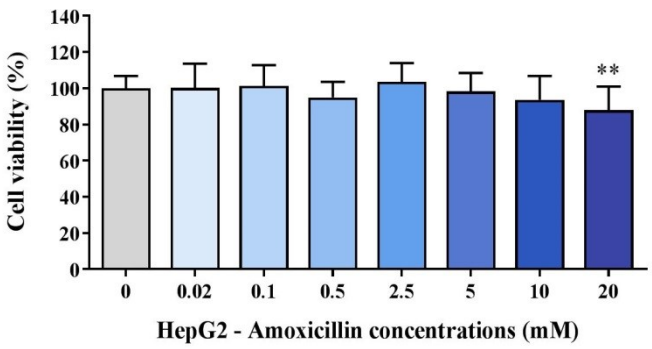

Figure 9 ***Effect of AMO on cell viability assessed by MTT assay in HepG2 cells.*** Cultured cells were treated with increasing concentrations of AMO (0.02-20 mM) or were left untreated (0 mM / controls). Results are expressed as mean ± SD from three independent experiments. Sextuplicates were made for each concentration in each experiment.
** $p < 0.01$ vs. control.

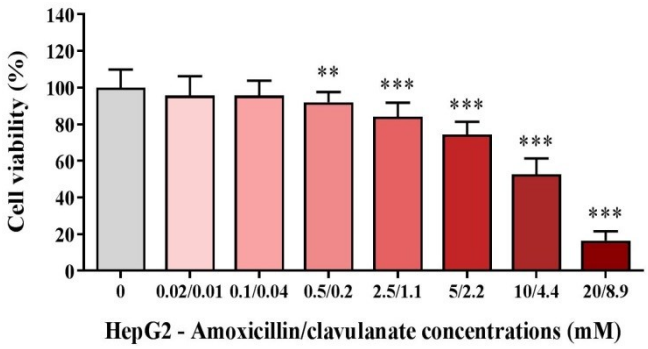

Figure 10 ***Effect of AMO/CLA on cell viability assessed by MTT assay in HepG2 cells.*** Cultured cell were treated with increasing concentrations of AMO/CLA (0.02/0.01-20/8.9 mM) or were left untreated (0 mM / controls). Results are expressed as mean ± SD from three independent experiments. Sextuplicates were made for each concentration in each experiment.
** $p < 0.01$ vs. control, *** $p < 0.001$ vs. control.

The results for Upcyte cells are shown for donor 10-03 and 422A-03 separately. The results for Upcyte cells (10-03) are summed up in Figure 11 for AMO and Figure 12 for AMO/CLA. Regarding AMO, no significant decrease was observed. On the contrary, a non-significant slight increase in cell viability was seen at lower concentrations. Regarding AMO/CLA, a significant increase was seen again in cells treated with low concentrations of 0.1/0.04 mM and 0.5/0.2 mM, whereas a reduction in cell viability was seen at the two highest concentrations (cell viability of 80 % at 10/4.4 mM and 40 % at 20/8.9 mM), which were excluded for further experiments.

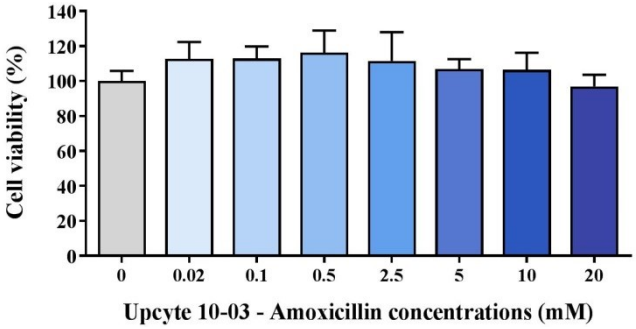

Figure 11 ***Effect of AMO on cell viability assessed by MTT assay in Upcyte cells 10-03.*** Cultured cell were treated with increasing concentrations of AMO (0.02-20 mM) or were left untreated (0 mM / controls). Results are expressed as mean ± SD from sextuplicates from one experiment.

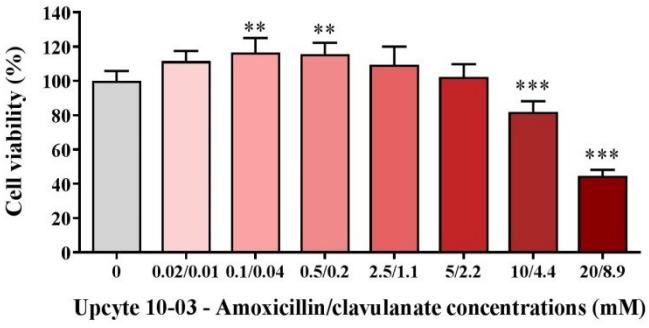

Figure 12 ***Effect of AMO/CLA on cell viability assessed by MTT assay in Upcyte cells 10-03.*** Cultured cell were treated with increasing concentrations of AMO/CLA (0.02/0.01-20/8.9 mM) or were left untreated (0 mM / controls). Results are expressed as mean ± SD from sextuplicates from one experiment.
** $p < 0.01$ vs. control, *** $p < 0.001$ vs. control.

The results for Upcyte cells (422A-03) are shown in Figure 13 for AMO and in Figure 14 for AMO/CLA. Considering previous results from Upcyte (10-03), a narrower range of concentrations was used. Treatment was performed with AMO at the concentrations from 0.5 to 20 mM, or with AMO/CLA at the concentrations from 0.5/0.2 to 20/8.9 mM. No significant changes were observed in samples treated with AMO. Regarding AMO/CLA, a significant decrease was seen at the three highest concentrations (5/2.2, 10/4.4 and 20/8.9 mM). The two highest concentrations of 10/4.4 mM and 20/8.9 mM with very low cell viabilities of 60 % and 10 %, respectively, were excluded for further experiments. Nevertheless, donor 422A-03 was not used for following evaluation of gene expression due to lack of time and complications with cell cultures.

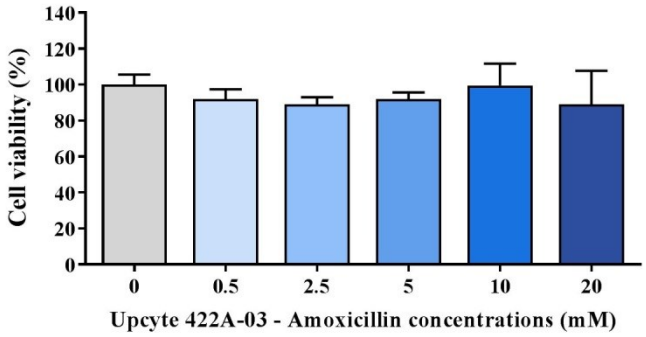

Figure 13 ***Effect of AMO on cell viability assessed by MTT assay in Upcyte cells 422A-03.*** Cultured cells were treated with increasing concentrations of AMO (0.5-20 mM) or were left untreated (0 mM / controls). Results are expressed as mean ± SD from quintuplicates from one experiment.

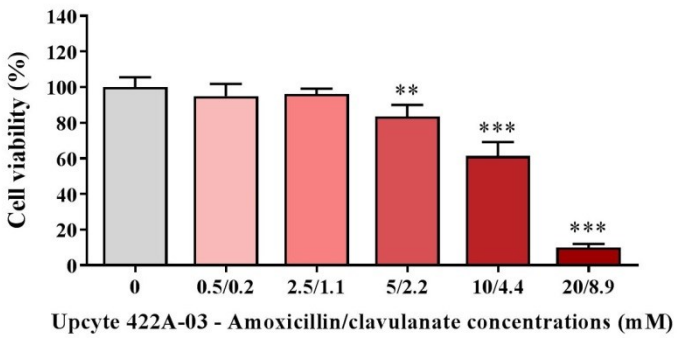

Figure 14 ***Effect of AMO/CLA on cell viability assessed by MTT assay in Upcyte cells 422A-03.*** Cultured cells were treated with increasing concentrations of AMO/CLA (0.02/0.01-20/8.9 mM) or were left untreated (0 mM / controls). Results are expressed as mean ± SD from quintuplicates from one experiment.
** $p < 0.01$ vs. control, *** $p < 0.001$ vs. control.

As expected, no effect of VALP (4 mM) on the viability of HepG2 and Upcyte cells (10-03 and 422A-03) was observed. This concentration was used according to previous study (Donato et al. 2016). The results of the MTT assays for HepG2 and both Upcyte donors are shown in Figure 15.

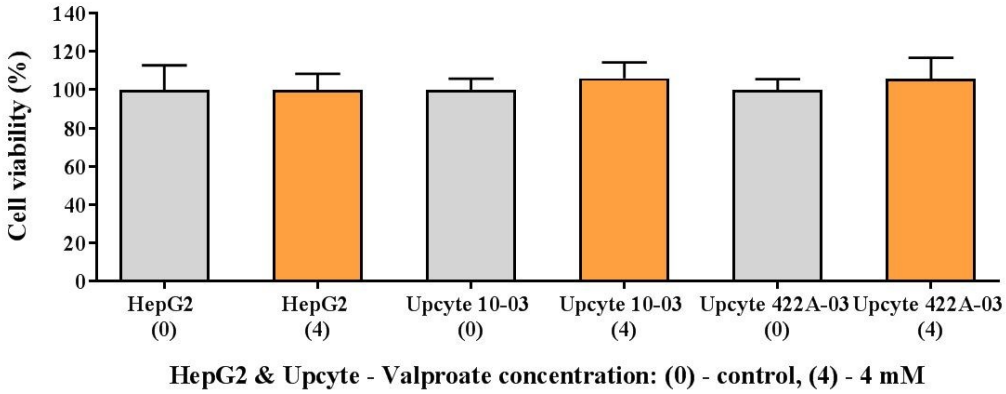

Figure 15 ***Effect of VALP on cell viability assessed by MTT assay in HepG2, Upcyte 10-03 and Upcyte 422A-03 cells.*** Cultured cells were treated with VALP (4 mM) or were left untreated (0 mM / controls). Results are expressed as mean ± SD from quintuplicates from one experiment.

6.2 Gene expression

The hypothesis is that the frequently prescribed antibacterial combination of AMO/CLA can influence BA synthesis, transport and homeostasis, as it happens with other well-known cholestatic drugs. In general, this hepatotoxic effect can be caused by several possible mechanisms, such as direct interference with the activity of BA transporters (for instance the inhibition of BSEP), detrimental polymorphisms in transporter genes or alterations in the regulation of gene expression (Donato et al. 2016, Morgan et al. 2010, Zollner et al. 2001). The last mentioned mechanism, altered regulation of gene expression by AMO/CLA, was chosen as the main hypothesis in this research project. For this reason, the mRNA levels of several important transporters, enzymes and NRs expressed in HepG2 and Upcyte cells were measured using q-RT-PCR after treatment with AMO, AMO/CLA or VALP.

Concerning the effect of AMO in HepG2 cells (Figure 16), gene expression was evaluated after treatment with two concentrations (0.5 mM and 2.5 mM) for 24 hours. Untreated cells were used as a negative control and cells treated with VALP (4 mM) for 24 hours were used as a positive control with demonstrated effects in gene expression (Donato et al. 2016). The only significant change was observed in the mRNA level of CYP7A1. The mRNA level of this rate-limiting enzyme important for *de novo* BA synthesis was decreased at both tested concentrations.

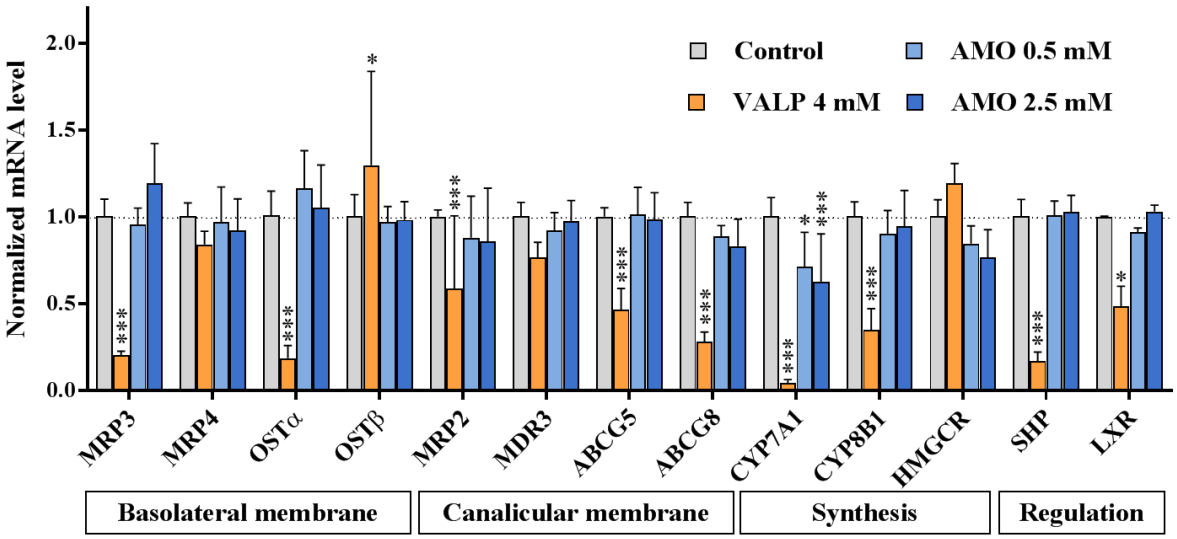

Figure 16 ***Effect of AMO on gene expression of hepatobiliary transporters, enzymes and nuclear receptors assessed by q-RT-PCR in HepG2 cells.*** Cultured cells were treated with AMO (0.5 mM and 2.5 mM), VALP (4 mM) or were left untreated (0 mM / controls). Results are expressed as mean ± SD from three independent experiments.
* $p < 0.05$ vs. control, ** $p < 0.01$ vs. control, *** $p < 0.001$ vs. control.

Regarding the effect of AMO/CLA in HepG2 cells (Figure 17), gene expression was tested after incubation with two concentrations (0.5/0.2 mM and 2.5/1.1 mM) for 24 hours. Untreated cells were used as a negative control and cells treated with VALP (4 mM) for 24 hours were used as a positive control. Among basolateral transporters, a significant induction of OSTβ (both uptake and efflux of BAs) and a non-significant mild induction of MRP4 (efflux of conjugated BAs) expression were seen at the highest concentration (2.5/1.1 mM). Among canalicular transporters, alterations in MRP2, MDR3 and ABCG8 were observed. A significant induction of MRP2 (efflux of conjugated BAs and bilirubin) expression was seen at the highest concentration (2.5/1.1 mM), whereas MRP2 induction at 0.5/0.2 mM AMO/CLA was not significant. The expression of MDR3 (efflux of phospholipids) was slightly decreased at both concentrations, and a significant inhibition of ABCG8 expression was observed at the highest concentration (2.5/1.1 mM). The significant decreases in the expression of CYP7A1 and CYP8B1 (BAs synthesis, both) were seen again at the highest concentration (2.5/1.1 mM). Regarding the two measured NRs, SHP expression was significantly induced at the highest concentration (2.5/1.1 mM), which corresponds with the decreased levels of CYP7A1 and CYP8B1 since SHP stops transcription of these genes (Chiang 2002).

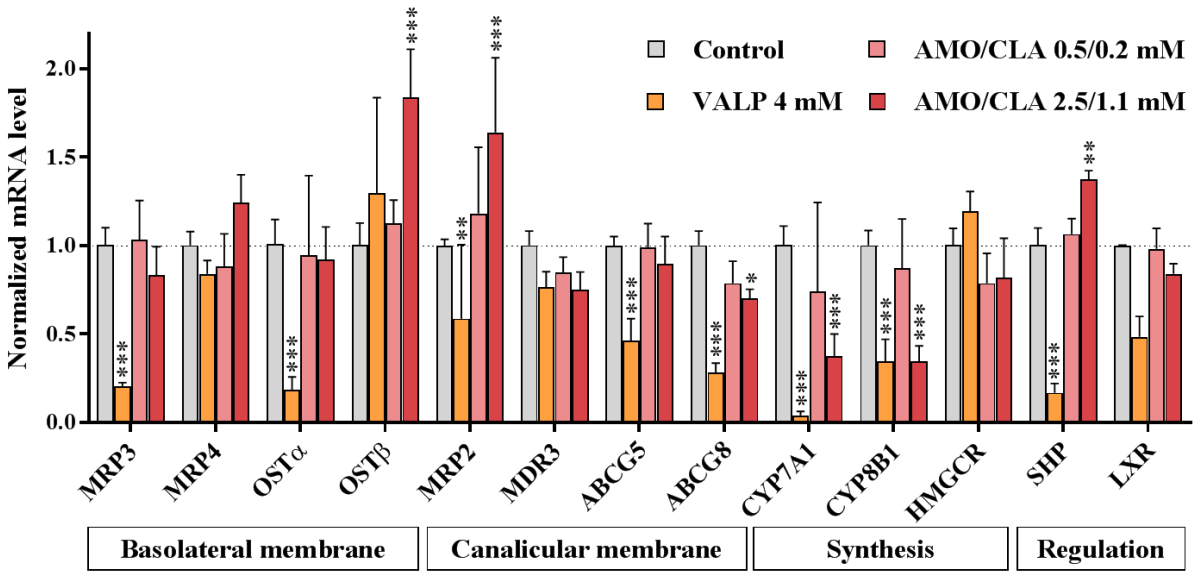

Figure 17 ***Effect of AMO/CLA on gene expression of hepatobiliary transporters, enzymes and nuclear receptors assessed by q-RT-PCR in HepG2 cells.*** Cultured cells were treated with AMO/CLA (0.5/0.2 mM and 2.5/1.1 mM), VALP (4 mM) or were left untreated (0 mM / controls). Results are expressed as mean ± SD from three independent experiments.
* $p < 0.05$ vs. control, ** $p < 0.01$ vs. control, *** $p < 0.001$ vs. control.

Compared with HepG2 cells, Upcyte cells comprise a better cellular model for testing hepatobiliary transporters due to ability to maintain NTCP and BSEP expression at higher levels than in HepG2 (Tolosa et al. 2016). Thus, the range of BA transporters tested in Upcyte cells was wider.

Regarding the effect of AMO in Upcyte 10-03 cells (Figure 18), the gene expression was evaluated after incubation with three concentrations (0.5, 2.5 and 5 mM) for 24 hours. Untreated cells were used as a negative control and cells treated with VALP (4 mM) for 24 hours were used as a positive control. The only significant effects were observed at the highest concentration of AMO (5 mM) on the expression of MRP2 and MDR3. Specifically, induced MRP2 (efflux of conjugated BAs and bilirubin) and MDR3 (efflux of phospholipids) expressions were observed.

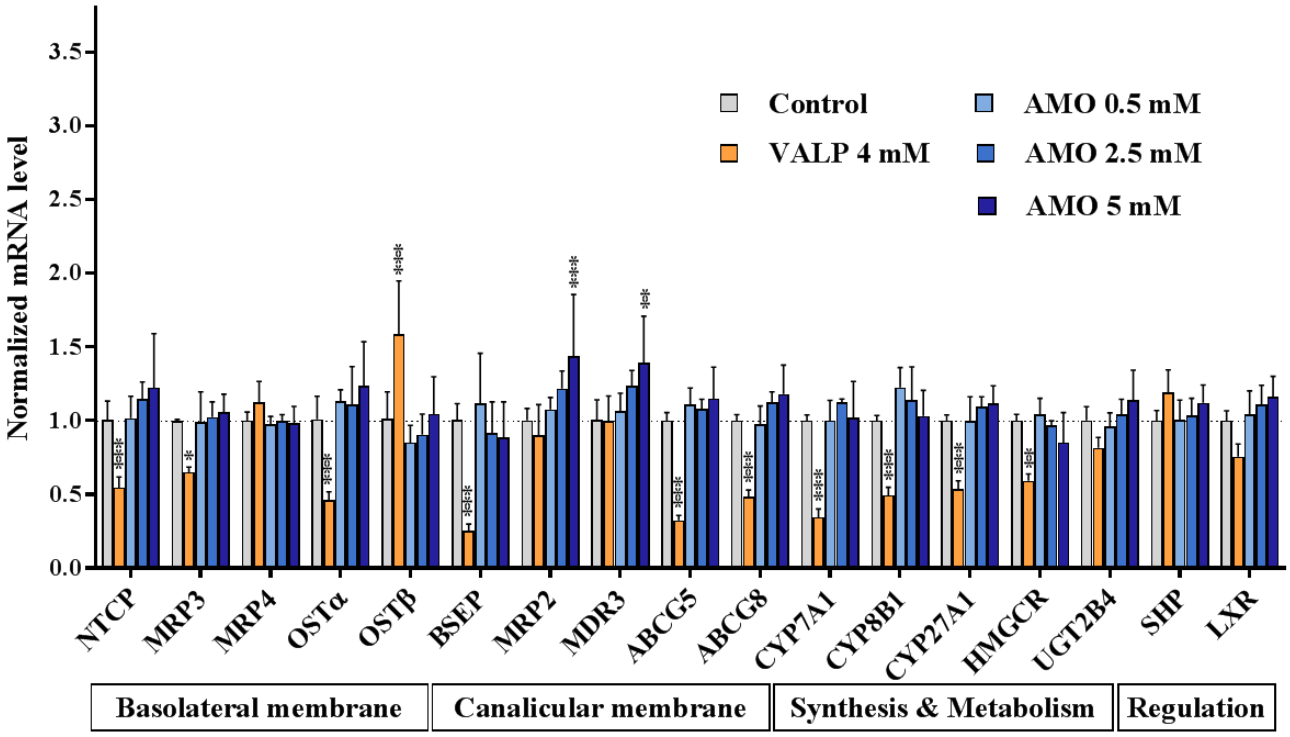

Figure 18 ***Effect of AMO on gene expression of hepatobiliary transporters, enzymes and nuclear receptors assessed by q-RT-PCR in Upcyte 10-03 cells.*** Cultured cells were treated with AMO (0.5, 2.5 and 5 mM), VALP (4 mM) or were left untreated (0 mM / controls). Results are expressed as mean ± SD from two independent experiments.
* $p < 0.05$ vs. control, ** $p < 0.01$ vs. control, *** $p < 0.001$ vs. control.

However, when the cells from the same donor (10-03) were treated with AMO/CLA combinations (0.5/0.2, 2.5/1.1 and 5/2.2 mM) for 24 hours (Figure 19), the effect on the expression of BA transporters, enzymes and NRs was much more widespread and extensive than with AMO alone (Figure 18). This was in agreement with the higher occurrence of DILI after AMO/CLA exposure than after AMO alone (deLemos et al. 2016).

Among basolateral transporters, the expression of NTCP (uptake of conjugated BAs) was significantly inhibited at the two highest concentrations of AMO/CLA (2.5/1.1 and 5/2.2 mM), which could act as an adaptive mechanism triggered by accumulated BAs within hepatocytes. A significant decrease in expression of OSTα was observed at the same concentrations, but the expression of OSTβ was significantly induced. The OSTα-OSTβ is a complex of two interdependent proteins involved in either uptake or efflux of BAs depending on the electrochemical gradient. OSTα works equimolecularly with OSTβ and, therefore, the changed levels of each subunit could lead to a decreased activity of this heterodimeric transporter (Ballatori et al. 2010).

Concerning canalicular transporters, the expression of BSEP (efflux of conjugated BAs) was also significantly decreased at the two highest concentrations (2.5/1.1 and 5/2.2 mM), which could represent a key mechanism for accumulation of BAs within hepatocytes and cholestasis provoked by AMO/CLA. A significant inhibition was also seen for ABCG5 and ABCG8 (efflux of cholesterol) at the same concentrations, thus cholesterol, the substrate for *de novo* BA synthesis, could be accumulated as well. Each tested concentration of AMO/CLA (0.5/0.2, 2.5/1.1 and 5/2.2 mM) induced the expression of MRP2 (efflux of conjugated BAs and bilirubin), a significant effect was seen at the two highest concentrations.

Among enzymes important for BA synthesis and metabolism, each tested CYP showed a significant inhibition of its gene expression. This could represent an adaptive mechanism triggered by high intracellular BA levels. The expression of CYP7A1 (the classic biosynthetic pathway for BAs) was significantly decreased at all three concentrations, CYP8B1 (the classic and alternative biosynthetic pathways for BAs) was significantly decreased at the two highest concentrations and CYP27A1 (mainly the alternative biosynthetic pathway for BAs) was significantly inhibited at the highest concentration of 5/2.2 mM and non-significantly at the concentration of 2.5/1.1 mM.

Regarding NRs, the expression of SHP showed a significant induction at the two highest concentrations (2.5/1.1 and 5/2.2 mM). The function of SHP consists in stopping the transcription of CYP7A1 and CYP8B1, thus *de novo* BA synthesis is suppressed. This effect represents a negative feedback for BA biosynthetic pathway. Specifically, BAs firstly activate FXR, which subsequently activates SHP (Chiang 2002). On the contrary, the expression of LXR was significantly inhibited at the highest concentration (5/2.2 mM). The LXR function in mice and rats was reported to induce CYP7A1 (Lehmann et al. 1997). However, the LXR function in humans is still not completely elucidated (Chiang 2004).

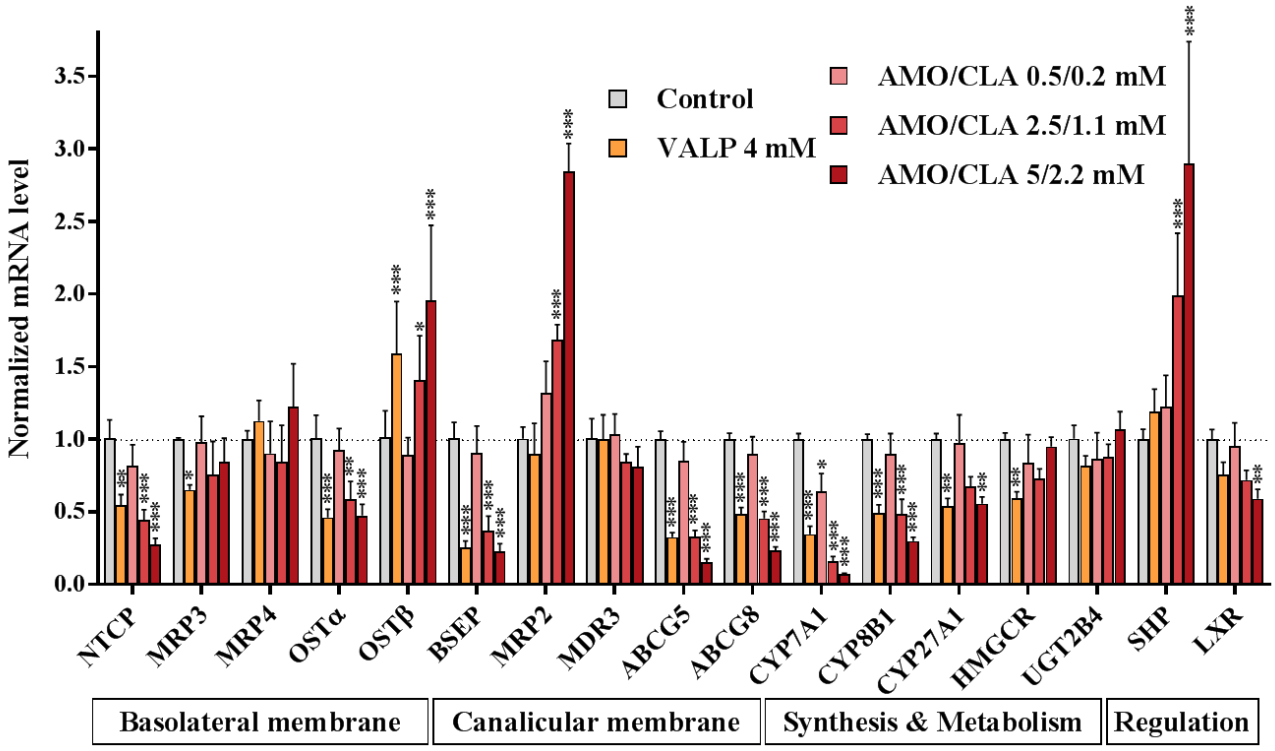

Figure 19 ***Effect of AMO/CLA on gene expression of hepatobiliary transporters, enzymes and nuclear receptors assessed by q-RT-PCR in Upcyte 10-03 cells.*** Cultured cells were treated with AMO/CLA (0.5/0.2, 2.5/1.1 and 5/2.2 mM), VALP (4 mM) or were left untreated (0 mM / controls). Results are expressed as mean ± SD from two independent experiments.
* $p < 0.05$ vs. control, ** $p < 0.01$ vs. control, *** $p < 0.001$ vs. control.

Under ongoing cholestasis, accumulated BAs could also impact the gene expression level of genes involved in BA homeostasis (Goodwin et al. 2000). To specifically evaluate this aspect in our *in vitro* model, HepG2 cells were treated with a mixture of BAs for 24 hours. The relative concentrations of the major BA species in this mixture was similar to that described for humans and can be found in the chapter 5.3.2 (Treatment with studied compounds).

HepG2 cells were treated with the mixture of BAs and the mRNA levels of key BA transporters, enzymes and NRs were compared with untreated cells (negative control) (Figure 20). Measured values showed four significant alterations in gene expression. First, the expression of OSTα and OSTβ was significantly induced. Another important change was observed in the expression of CYP7A1, the rate-limiting enzyme in the classic biosynthetic pathway for BAs. More specifically, the mRNA level of CYP7A1 was significantly decreased, which agrees with a significant induction of SHP. The role of SHP on CYP7A1 as a negative feedback triggered by accumulated BAs was reported before (Chiang 2002) and possibly represents an adaptive mechanism to cope with the increasing concentration of intracellular BAs.

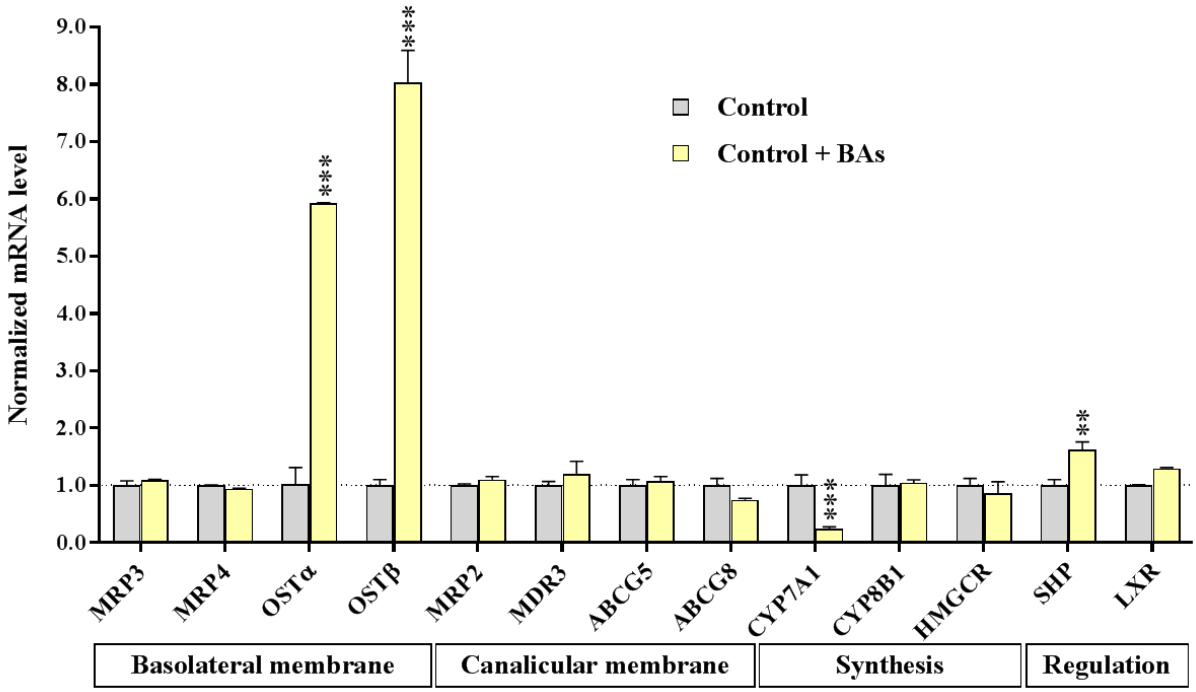

Figure 20 ***Effect of BAs on gene expression of hepatobiliary transporters, enzymes and nuclear receptors assessed by q-RT-PCR in HepG2 cells.*** Cultured cells were treated with the mixture of BAs or were left untreated (0 mM / controls). Results are expressed as mean ± SD from triplicates from one experiment.
* $p < 0.05$ vs. control, ** $p < 0.01$ vs. control, *** $p < 0.001$ vs. control.

Secondly, HepG2 cells were treated together with the mixture of BAs and two concentrations of AMO (0.5 and 2.5 mM), AMO/CLA (0.5/0.2 and 2.5/1.1 mM) or VALP (4 mM). The mRNA levels of key BA transporters, enzymes and NRs were expressed as fold-change to the level observed in the cells treated with BAs alone (Figure 21). Regarding basolateral transporters, a significant inhibition of MRP3 (efflux

of conjugated BAs) expression was seen at the AMO/CLA concentration 2.5/1.1 mM. The expression of MRP4 (efflux of conjugated BAs) was significantly inhibited at the AMO concentrations of 0.5 and 2.5 mM and non-significantly at 2.5/1.1 mM of AMO/CLA. This ability to inhibit the expression of efflux transporters MRP3 and MRP4 may represent one of the pro-cholestatic mechanisms of AMO/CLA; however, this effect was not unequivocally seen in results for AMO and AMO/CLA in HepG2 cells (Figure 16 and 17). The expression of OSTα subunit was significantly inhibited at the highest AMO/CLA concentration (2.5/1.1 mM). Regarding canalicular transporters, the expression of MDR3 (efflux of phospholipids) was significantly and non-significantly inhibited at the AMO/CLA concentrations 2.5/1.1 and 0.5/0.2 mM, respectively. The mRNA levels of the efflux transporters for cholesterol, ABCG5 and ABCG8, were non-significantly decreased. Concerning tested enzymes and NRs, the mRNA levels of CYP7A1 and CYP8B1 were decreased at all tested concentrations, through which *de novo* synthesis of BAs is slowed down. A significant inhibition of HMGCR (biosynthesis of cholesterol) expression was seen at all tested concentrations of AMO/CLA and the highest concentration of AMO (2.5 mM). Unlike previous result in HepG2 cells not exposed to BAs (Figure 16 and 17), the mRNA levels of SHP was unchanged or decreased non-significantly after treatment with AMO/CLA.

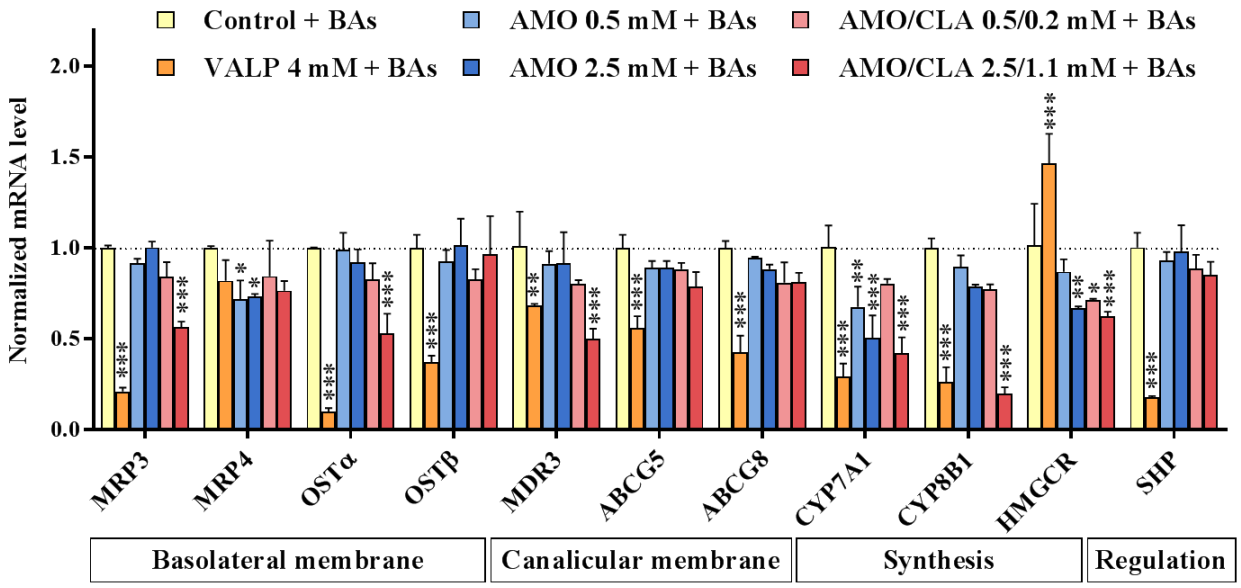

Figure 21 ***Effect of BAs and AMO, AMO/CLA or VALP on gene expression of hepatobiliary transporters, enzymes and nuclear receptors assessed by q-RT-PCR in HepG2 cells.*** Cultured cells were treated together with the mixture of BAs and AMO (0.5 and 2.5 mM), AMO/CLA (0.5/0.2 and 2.5/1.1 mM) or VALP (4 mM) or were treated with the mixture of BAs only (control). Results are expressed as mean ± SD from triplicates from one experiment.
* $p < 0.05$ vs. control, ** $p < 0.01$ vs. control, *** $p < 0.001$ vs. control.

When HepG2 cells were exposed to AMO, without added extracellular BAs (Figure 16), MRP4 and HMGCR were not significantly repressed; and when they were exposed to AMO/CLA, without added extracellular BAs (Figure 17), MRP3, OSTα, MDR3 and HMGCR were not significantly repressed. On the contrary, AMO/CLA, when combined with BAs, did not induce the level of OSTβ and SHP, likely because they are already induced by the added BAs (Figure 20). Therefore, it can be concluded that, when the cholestatic condition of high plasma BA levels is mimicked, the perturbation of these drugs on BA related genes is wider and more extensive.

6.3 Protein analysis

As Upcyte cells allow evaluation of more key hepatobiliary transporters than HepG2 cells (Tolosa et al. 2016), this cellular model was used for protein detection. After treatment with AMO (5 mM), AMO/CLA (5/2.2 mM) and VALP (4 mM) for 24 and 48 hours, total protein was isolated from cells and quantified. Then, samples with equivalent amount of total protein (40 μg) were separated using SDS-PAGE. The transferred bands of proteins were detected on PVDF membranes as described in the chapter 5.3.11 (Western blot). These experiments were integrated into this thesis in order to test if the changes observed at the mRNA levels of two crucial BA protein transporters (NTCP and BSEP) translate at the functional protein level.

The NTCP is a basolateral transporter which imports conjugated BAs from portal blood into the hepatocyte (Hagenbuch and Dawson 2004). The molecular mass of NTCP is stated to be 38.1 kDa (Pontén et al. 2008). The protein was detected by SDS-PAGE with subsequent immunoblotting. A sample of human liver from Biobank of cryopreserved livers (Hospital La Fe, Valencia, Spain), with previously confirmed presence of NTCP by researchers from Hospital La Fe, was included as a positive control. Besides NTCP, the detection of glyceraldehyde 3-phosphate dehydrogenase (GAPDH) was used as an internal normalization control. The results are summarized in Figure 22. The problematic unexpectedness was seen in detection of double bands, especially in the samples of AMO and AMO/CLA. This could be a result of either post-translational modifications or poor specificity of the used antibody. However, achieved results showed that the protein expression levels of NTCP were lower after treatment with AMO/CLA 5/2.2 mM at both tested time periods (24 and 48 hours),

which agreed with the decreased mRNA expression level after 24 hours of treatment. The cells treated with AMO 5 mM for 48 hours showed lower protein expression as well, nevertheless, the gene expression analysis at this time period was not performed. The parallel inhibition of mRNA and protein expression of NTCP could represent an adaptive mechanism for accumulated BAs within hepatocytes or could indicate a novel pro-cholestatic mechanism of AMO/CLA that would lead to higher circulating plasma levels of conjugated BAs. Unfortunately, the analysis of relative density for the individual protein bands has not been performed yet and therefore the results are expressed only as images captured after immunoblotting.

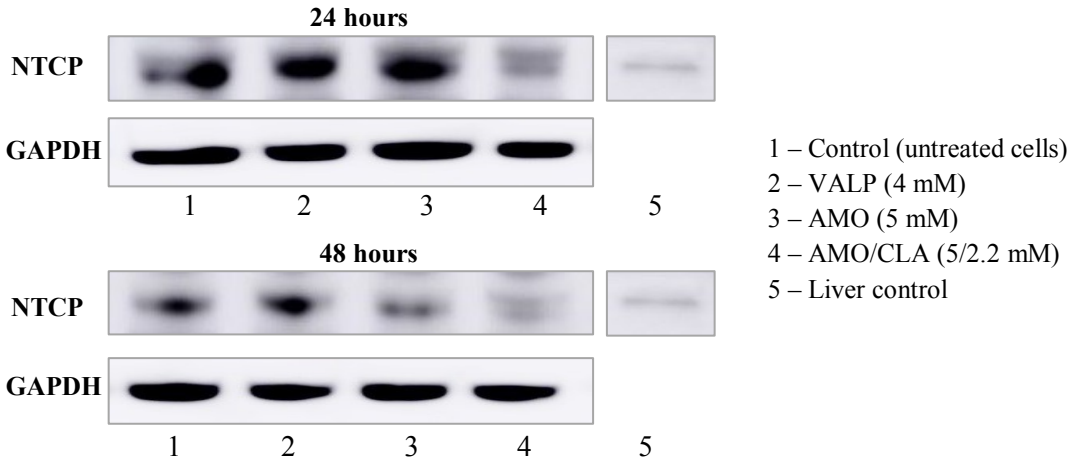

Figure 22 ***Effect of AMO, AMO/CLA or VALP on NTCP protein expression assessed by immunoblotting in Upcyte 10-03 cells.*** Cultured cells were treated with AMO (5 mM), AMO/CLA (5/2.2 mM) or VALP (4 mM) for 24 and 48 hours or were left untreated (0 mM / controls). The expression of NTCP (38.1 kDa) was assessed by Western blot and subsequent immunoblotting. GAPDH was used as an internal normalization control.

The BSEP is a canalicular transporter for which the efflux of conjugated BAs into the bile canaliculi is characteristic (Dawson et al. 2009). The molecular mass of BSEP is stated to be 146.4 kDa (Pontén et al. 2008). Compared to NTCP, the mass of BSEP is higher and even after using a gel with lower polyacrylamide concentration (7.5%) this protein was not detected in any sample. However, especially in the sample of human liver control from Biobank of cryopreserved livers (Hospital La Fe, Valencia, Spain), with previously confirmed expression of BSEP by researchers from Hospital La Fe, an intense band was visualized in the loading well of the stacking gel. This could mean protein aggregation or precipitation at the entry of the stacking gel.

Other potential explanation could be a low specificity of the used antibody, or low sensitivity requiring higher levels of expressed protein, which would limit the detection in the samples with decreased mRNA levels, as expected in AMO/CLA samples (Figure 19). For this reason, the method needs optimization. The image of the processed membrane is presented for illustrative purposes in Figure 23.

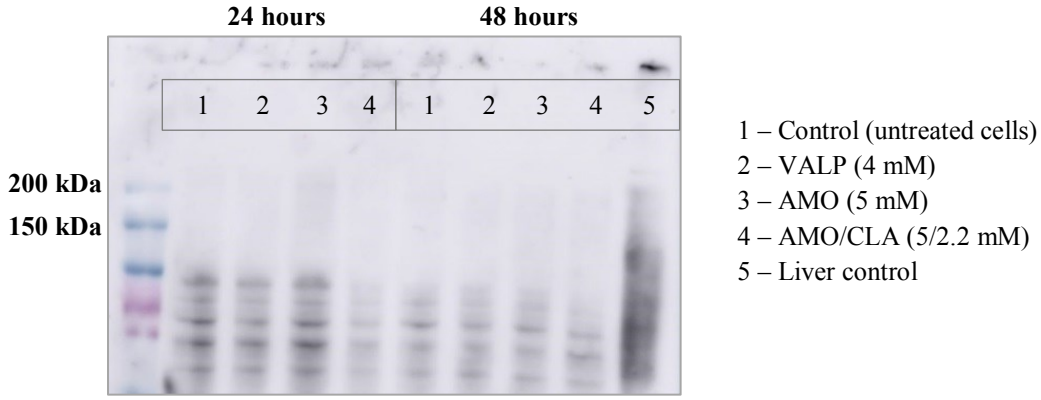

Figure 23 ***Illustrative image of membrane from Western blot after incubation with BSEP antibody.*** Unfortunately, the protein of BSEP (146.4 kDa) was not detected in any sample.

6.4 Cell microscopy

In order to document the appearance and morphology of the cultured cells treated with cholestatic drugs and BAs, inverted light microscope Leica was used.

Firstly, HepG2 cells (Figure 24) were treated with increasing concentrations of AMO/CLA (0.02/0.01, 0.1/0.04, 0.5/0.2, 2.5/1.1, 5/2.2, 10/4.4 and 20/8.9 mM) for 24 hours or were left untreated (0 mM / control) in 96-well plates. Images were captured just before the MTT assay. The noticeable decrease in cell viability and changes in cell morphology were evident from the concentration of 2.5/1.1 mM and higher.

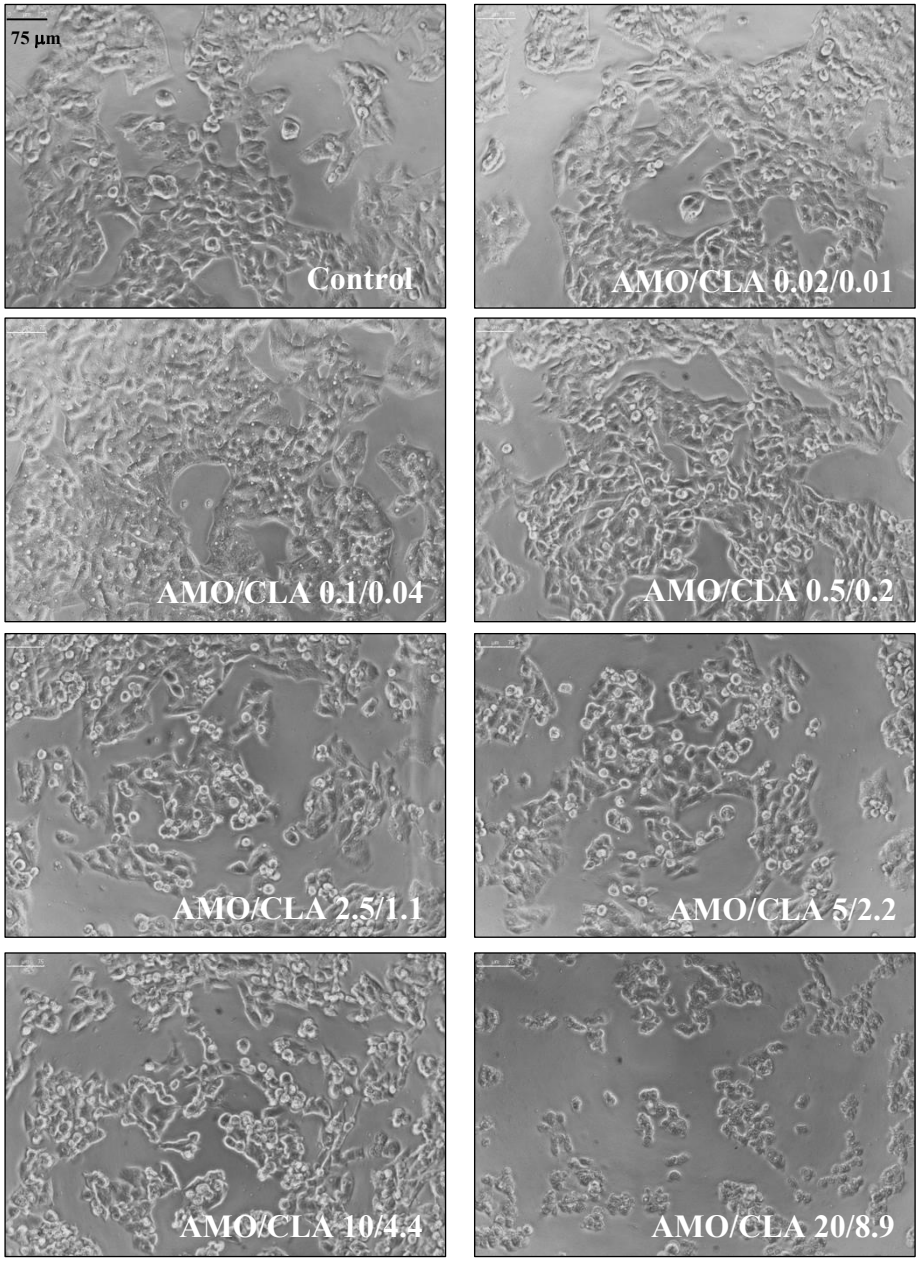

Figure 24 ***Representative images of HepG2 cells treated with AMO/CLA captured using digital microscopy.*** Cultured cells were treated with increasing concentrations of AMO/CLA (0.02/0.01-20/8.9 mM) or were left untreated (0 mM / control). The used magnification was 75×.

Secondly, the images of human Upcyte 10-03 hepatocytes (Figure 25) were captured using digital microscopy as well. Cells were treated with increasing concentrations of AMO/CLA (0.02/0.01, 0.1/0.04, 0.5/0.2, 2.5/1.1, 5/2.2, 10/4.4 and 20/8.9 mM) for 24 hours or were left untreated (0 mM / control) in 96-well plates with one collagen layer. Images were captured just before the MTT assay. The noticeable change of cell morphology and decreased cell viability were observed at the two highest concentration of AMO/CLA (10/4.4 and 20/8.9 mM).

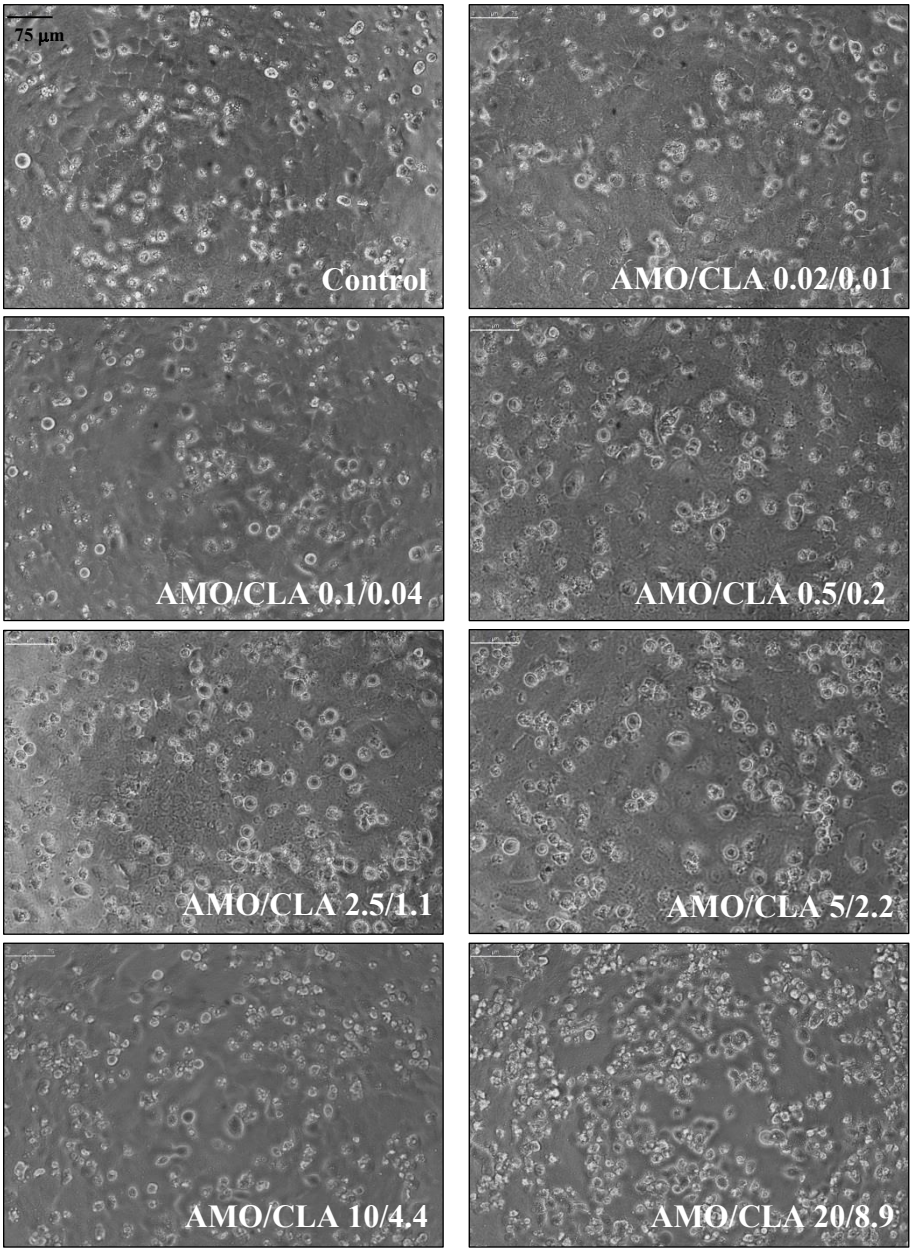

Figure 25 ***Representative images of Upcyte 10-03 cells treated with AMO/CLA captured using digital microscopy.*** Cultured cells were treated with increasing concentrations of AMO/CLA (0.02/0.01-20/8.9 mM) or were left untreated (0 mM / control). The used magnification was 75×.

The visualization of HepG2 cells treated with the mixture of BAs together with AMO (0.5 and 2.5 mM) or AMO/CLA (0.5/0.2 and 2.5/1.1 mM), or treated only with AMO or AMO/CLA, is shown in Figure 26. The images of HepG2 cells treated together with the mixture of BAs and VALP (4 mM) or only with the mixture of BAs or VALP (4 mM) are presented in Figure 27. After 24 hours of incubation with tested compounds in 24-well plates, the images were captured using digital microscopy.

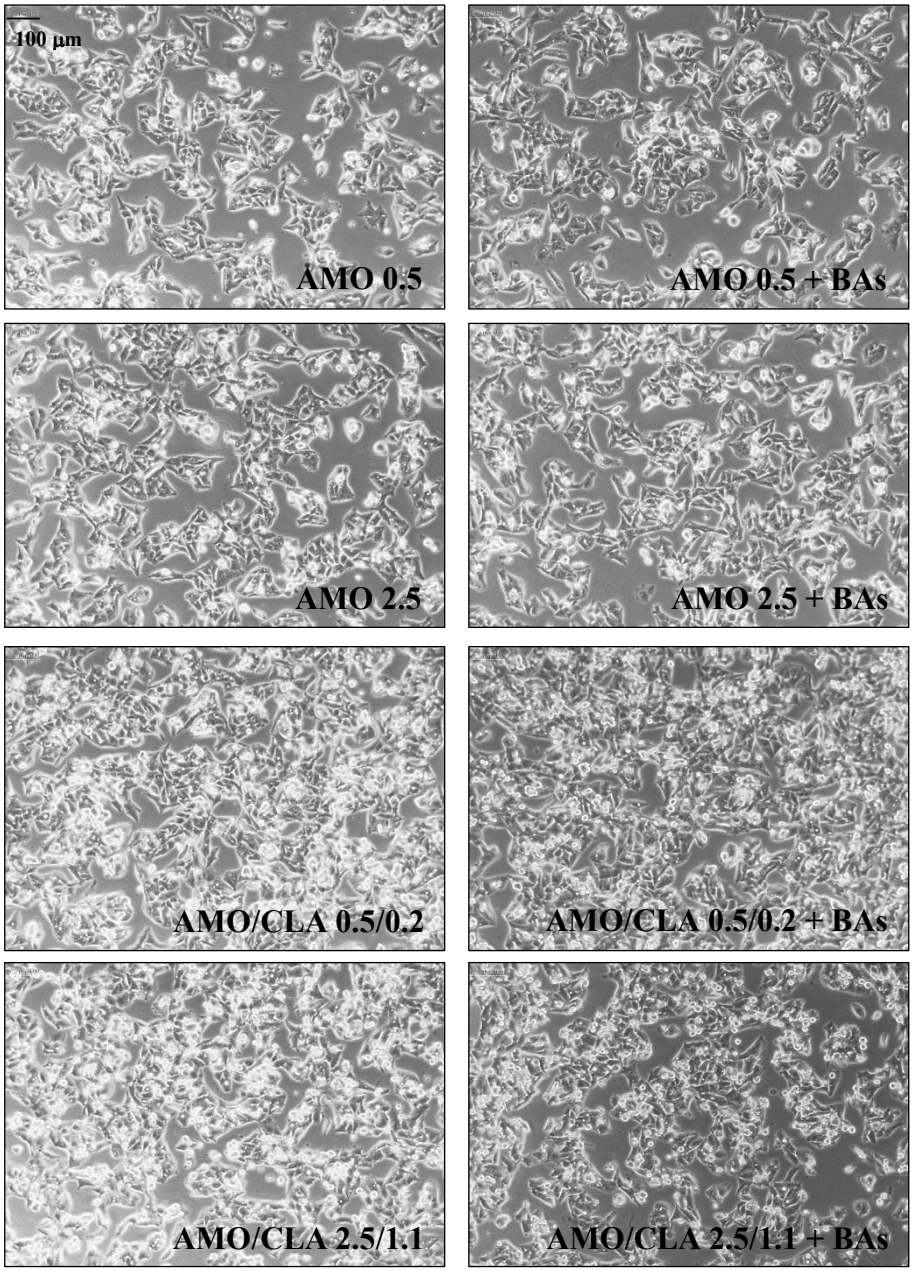

Figure 26 ***Representative images of HepG2 cells treated only with AMO or AMO/CLA or in combination with the mixture of BAs captured using digital microscopy.*** Cultured cells were treated with selected concentrations of AMO (0.5 and 2.5 mM) or AMO/CLA (0.5/0.2 and 2.5/1.1 mM) or were treated in combination of AMO or AMO/CLA with the mixture of BAs. The used magnification was 100×.

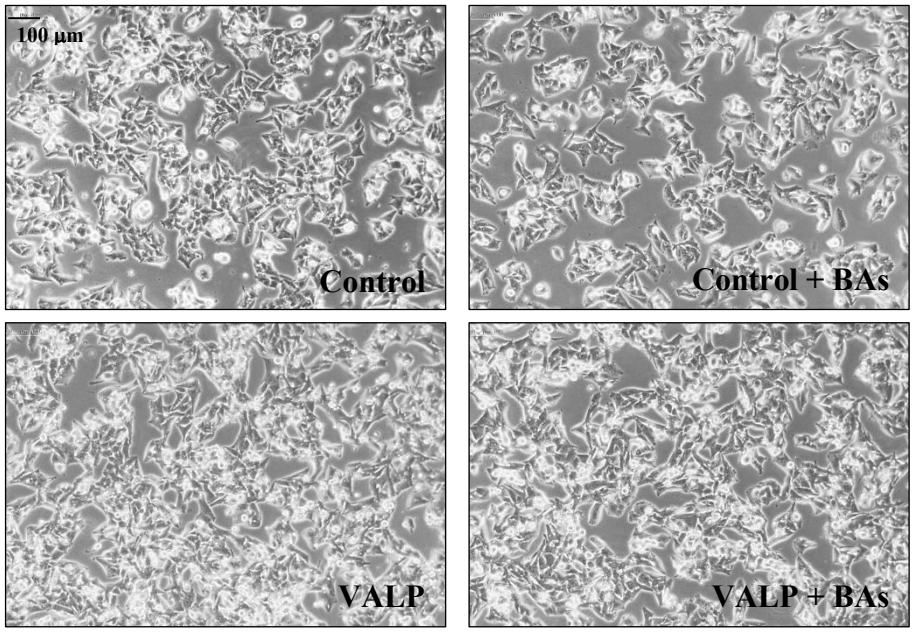

Figure 27 ***Representative images of HepG2 cells treated with VALP, combination of VALP and the mixture of BAs or BAs only captured using digital microscopy.*** Cultured cells were treated with selected concentration of VALP (4 mM), the mixture of BAs or were treated together with VALP and the mixture of BAs. The untreated cells served as control. The used magnification was 100×.

Digital microscopy projected on a connected computer is a useful method for quick visual assessment of cultured cells. This type of microscopy, which uses an inverted light microscope, also provides easy digital documentation of cultured cell morphology using images captured with a built-in camera. Nevertheless, additional methods (e.g. fluorescence microscopy) would be needed for further examination of specific functional alterations in treated cells; therefore presented images are only intended to provide representative documentation of cell morphology and viability.

7 DISCUSSION

AMO/CLA is the most frequent cause of diagnosed cases of idiosyncratic DILI as reported by the American (Chalasani et al. 2008), Spanish (Andrade et al. 2005) and Icelandic (Björnsson et al. 2013) DILI research networks. The liver injury caused by AMO/CLA is classified as cholestatic DILI in the majority of cases and less frequently as mixed (the combination of cholestatic and hepatocellular damages) or hepatocellular type of DILI (Lucena et al. 2006, Robles et al. 2010). However, each idiosyncratic response represents a challenge for medical doctors and life science researches because it develops only in a small fraction of treated patients who likely are susceptible individuals; and especially preclinical tests of new drugs are not reliably able to detect potential idiosyncratic side effects (Leise et al. 2014, Petrov et al. 2018). Nowadays, there are no cell models able to mimic this idiosyncratic response and therefore testing AMO/CLA in hepatic cell lines and cultured hepatocytes may hide limitations. In this presented diploma thesis, the pivotal aim was to evaluate molecular mechanisms involving alterations in gene expression of several crucial BA transporters, enzymes and NRs, and thereby shed light onto the research field of DILI by AMO/CLA.

The MTT assay was initially designed to determine non-cytotoxic concentrations for further treatments of two hepatocellular models – HepG2 and Upcyte cells. According to the results achieved from the MTT assays, selected non-cytotoxic AMO concentrations of 0.5 and 2.5 mM are approximately 25-fold and 125-fold, respectively, higher than the observed common therapeutic maximum plasma concentration (C_{max}), which for amoxicillin is reported to be 7.19 μg/mL (SÚKL 2017). Selected CLA concentrations of 0.2, 1.1 and 2.2 mM are approximately 20-fold, 90-fold and 180-fold, respectively, above the common therapeutic C_{max} of clavulanic acid which is 2.4 μg/mL (SÚKL 2017). In acute hepatotoxicity assays, 100-fold C_{max} is usually used for distinction between safe and toxic drug effects (Tolosa et al. 2018), and therefore, the range of concentrations selected here are in agreement with the current procedures of *in vitro* toxicology. The evaluation of the effects of AMO/CLA on gene expression was carried out at non-cytotoxic concentrations which prevents from mixed side effects triggered by the activation of necrotic and apoptotic pathways at cytotoxic concentrations.

In this study, two hepatocellular models were used. The first cellular model, HepG2 cells, represents a basic and relatively easy-handle standard for hepatotoxicity assessment, but several limitations are connected with HepG2 (Fernández-Murga et al. 2018).

Unfortunately, some of the crucial hepatobiliary transporters and metabolic enzymes are expressed at negligible levels or not expressed at all in HepG2. The mRNA expression levels of the basolateral transporter NTCP, the canalicular transporters BSEP, MDR3 and the BA synthesis enzyme CYP8B1 are expressed at a much higher level in Upcyte cells, and especially when plated in double-collagen sandwich configuration, the cells maintain typical polarised morphology as well as BA synthesis and transport pathways (Levy et al. 2015, Tolosa et al. 2016). For these reasons and the more hepatic-like phenotype, I have considered the Upcyte cells to be a more suitable cellular model for describing the molecular mechanisms of cholestasis induced by AMO/CLA.

VALP was used as a control drug with hepatotoxic side effects (Brunton et al. 2011). Despite its influence on the gene expression levels of key hepatobiliary transporters, enzymes and NRs have been evaluated recently by researchers from the same institution where this diploma thesis was performed (Donato et al. 2016) or by different research teams from other institutions (Chang et al. 2016), the precise mechanisms are still incompletely understood. One downside regarding the usage of VALP as a positive control is that VALP causes mainly hepatosteatosis and the pattern of changes in gene expression may differ between cholestatic and steatotic drugs (Donato et al. 2016). For this reason, I have not compared the effects between VALP and AMO or AMO/CLA. This drug was simply used as a positive control for monitoring the cell ability to react to the treatment, and furthermore, because of the availability of this compound. The interesting issue would be a comparison with other cholestatic drugs such as cyclosporine A or chlorpromazine (Mohi-ud-din and Lewis 2004, Sundaram and Björnsson 2017).

The gained outcomes from gene expression in Upcyte cells (10-03) indicated either probable routes for developing cholestasis or possible acquired adaptive responses which could result from ongoing accumulation of BAs. The repression of BSEP expression in human primary hepatocytes has already been connected with several drugs (e.g. glimepiride and lopinavir) leading to the disrupted BA homeostasis (Garzel et al. 2014) and the **repression of BSEP expression** was also seen in the Upcyte cells treated with AMO/CLA which was proved in this thesis. For other cholestatic drugs, such as cyclosporine A and pioglitazone, the direct interference with the BSEP transporter, which results in inhibition of its transport activity, was shown to be yet another possible cause for developing DILI (Morgan et al. 2010).

Another significantly **reduced expression** was observed on **ABCG5 and ABCG8**. These canalicular transporters excrete cholesterol and plant sterols from hepatocytes into the bile (Graf et al. 2003). The decreased levels of ABCG5 and ABCG8 may induce intracellular cholesterol accumulation. Cholesterol is a substrate for *de novo* synthesis of BAs. The increased amounts of cholesterol, possibly caused by ABCG5/8 reduction, and BAs, possibly caused by BSEP reduction, require several compensatory steps for maintaining BA and cholesterol homeostasis.

Regarding possible **adaptive responses**, the expression of BA biosynthesis enzymes was significantly inhibited. When repressed BSEP expression generates a strong accumulation of BAs within hepatocytes, *de novo* BA synthesis becomes redundant, and therefore levels of biosynthesis enzymes are decreased. More specifically, CYP7A1, CYP8B1 and CYP27A1 enzymes were found strongly inhibited in Upcyte cells treated with AMO/CLA. The transcription of CYP7A1 and CYP8B1 is regulated by SHP. Firstly, SHP is upregulated by the BA sensor FXR, and then secondly SHP stops CYP7A1 and CYP8B1 transcription (Chiang 2002, Goodwin et al. 2000). This hypothesis is supported by the finding that the SHP levels were strongly increased. The expression of FXR has not been measured, but alterations in the mRNA or protein levels of this NR are not expected; rather it is the activation of the intracellular FXR receptor by binding to agonistic BAs what triggers the signalling events leading to transcriptional activation of the SHP gene.

Among basolateral transporters, the **NTCP expression was significantly inhibited** in Upcyte cells treated with AMO/CLA which could indicate another adaptive mechanism to avoid the entry of more BAs into hepatocytes possibly triggered by BA-activation of FXR with subsequent role of SHP (Denson et al. 2001); or it could indicate a novel pro-cholestatic mechanism of AMO/CLA that would lead to higher circulating plasma levels of conjugated BAs. This effect was not observed in the samples treated with AMO alone. On the contrary, a non-significant increase in the NTCP level at the highest AMO concentration (5 mM) was observed.

The complex transporter OSTα-OSTβ evinced significant changes characterized by decrease of OSTα and increase of OSTβ levels. OSTα works equimolecularly with OSTβ and, therefore, the opposed regulation caused by AMO/CLA will lead to decreased activity of this heterodimeric transporter which will be limited by the reduced levels of OSTα. It is difficult to explain the pathway leading to this regulation without

further examination, but the upregulation of both OSTα-OSTβ proteins has previously been reported in other cholestatic conditions (Boyer et al. 2006).

Another **significant induction** was seen in the levels **of the transporter MRP2**, which ensures the efflux of conjugated BAs and bilirubin, but also many drugs and exogenous agents (Konig et al. 1999). The same effect of induction was observed with other cholestatic drugs (e.g. cyclosporine A and chlorpromazine) in the previous study on rat hepatocytes (Donato et al. 2016). The MRP2 induction in Upcyte cells treated with AMO/CLA could be either an adaptive response to deal with accumulated BAs or a process to dispose the absorbed drugs. However, the same effect of MRP2 induction was observed in the cells treated with AMO, where no direct cholestatic effects have been observed. On the other hand, another possible pro-cholestatic side effect caused by the induced MRP2 transporter is the BSEP *trans*-inhibition[3] by certain drug metabolites, such as estradiol and progesterone metabolites. These metabolites are firstly exported by MRP2 into the bile canaliculi, where can directly inhibit the BSEP transporter after reaching a threshold concentration (Pauli-Magnus and Meier 2006, Stieger et al. 2000). However, the BSEP *trans*-inhibition has been described for neither AMO nor CLA (Stieger et al. 2000), thus this mechanism needs further examination.

When comparing the effect of AMO and AMO/CLA on Upcyte cells, the possible mechanisms for developing cholestasis were mainly observed after treatment with AMO/CLA. These findings correspond with the higher frequency of DILI after AMO/CLA exposure in contrast to AMO alone (deLemos et al. 2016). The Upcyte cells treated with AMO showed significant changes only in expression of two canalicular transporters. The levels of MRP2 and MDR3 were increased after AMO treatment, which may contribute to the detoxifying and protective functions of hepatocytes. However, the drugs associated with the increased efflux conferred by MRP2 and MDR3 are reported to belong to antitumor drug class (Konig et al. 1999, Morita and Terada 2014). Another possibility of pro-cholestatic effect could be the BSEP *trans*-inhibition via induced MRP2, but there is no confirmed substrate specificity for AMO/CLA (Stieger et al. 2000). For further investigations about the effects of AMO, I suggest to treat cells with AMO for a longer time or use a time course experiment. Alternatively, the *trans*-inhibition can be tested by using a fluorescent BA analogue and microscopy.

---

[3] **BSEP *trans*-inhibition** = the inhibition of the canalicular BSEP transporter caused by certain drug metabolites presented in bile, the inhibition is done from canaliculus (Pauli-Magnus and Meier 2006)

In addition, a time course experiment in the Upcyte cells treated with AMO/CLA would be also applicable for deeper understanding of described possible mechanisms, because the mRNA levels may change over time. The pro-cholestatic effects may come first, whereas the adaptive response may be subsequent to the accumulation of BAs. This approach was initially included in the planned experiments, however, some complications with cell culturing unfortunately appeared and results could not be generated. Moreover, detailed protein analysis with Western blot and density quantification would be also required. The only plausible result from the performed Western blot analysis was the finding that the NTCP protein amount was also decreased after incubation with AMO/CLA. Another suggestion is to repeat experiments with the combination of AMO/CLA and a mixture of BAs in Upcyte hepatocytes and focus particularly on NTCP and BSEP. Ongoing cholestatic conditions were mimicked only in HepG2 cells and the effect of AMO and AMO/CLA appeared to be more extensive when co-incubated with BAs.

From a wider point of view, various mechanisms have been reported to be involved in the pathogenesis of drug-induced cholestasis and other types of DILI. The direct interference with transporters by drugs or their metabolites (Morgan et al. 2010) and the development of inflammation caused by ongoing cholestasis and accumulated BAs can play important roles in clinical, biochemical, but also in molecular characterisation of DILI. Regarding inflammation, the effect of pro-inflammatory cytokines such as tumor necrosis factor-α (TNF-α) and interleukin-6 (IL-6) has been previously evaluated and their ability to influence expression of hepatobiliary transporters has been proven to be significant (Le Vee et al. 2009). Regarding idiosyncrasy, certain genetic predispositions in HLA class II or mutations in BSEP and MDR3 genes has also been connected with higher risk for developing drug-induced cholestasis (Donaldson et al. 2010, Pauli-Magnus and Meier 2006). Last but not least, alterations in gene expression of hepatobiliary transporters and their altered regulation by NRs has been described to play a significant role in DILI and, more particularly, in drug-induced cholestasis (Donato et al. 2016, Le Vee et al. 2009, Pauli-Magnus and Meier 2006). In closing, I believe that this experimental diploma thesis could help to clarify some of the possible mechanisms of AMO/CLA DILI.

The achieved results of this experimental diploma thesis about the mechanisms of AMO/CLA DILI involving altered gene expression are summarized in Figure 28.

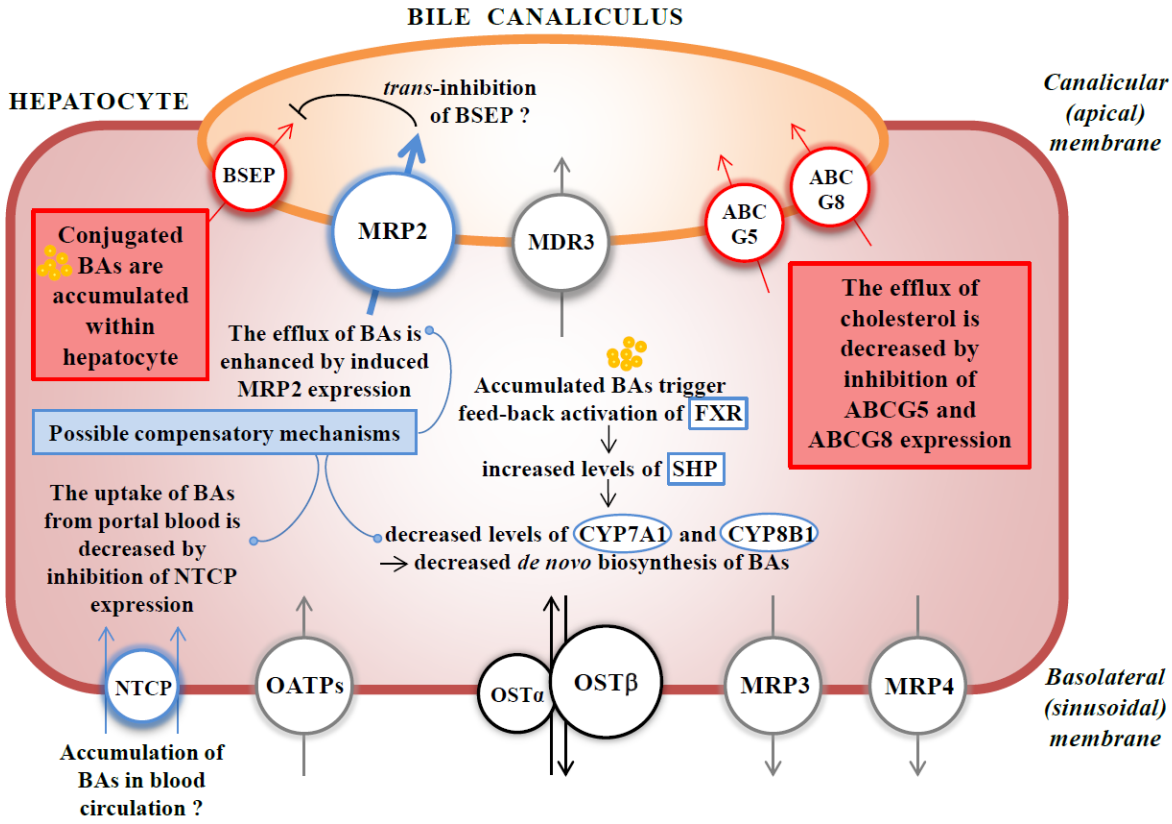

Figure 28 ***Schematic illustration of hepatobiliary transporters, enzymes and nuclear receptors and the description of possible mechanisms for DILI by AMO/CLA performed in human Upcyte hepatocytes.***

AMO/CLA inhibits **BSEP** and **ABCG5/8** (reduced red circles), which results in accumulation of BAs. This triggers feed-back activation of FXR, which will, in turn, inhibit BA uptake via **NTCP** (reduced blue circle) and BA synthesis (**CYP7A1** and **CYP8B1**) via **SHP**. AMO/CLA also induces canalicular BA and drug output via **MRP2** (increased blue circle), which could, in turn, *trans*-inhibit BSEP. Finally, AMO/CLA has opposed effects on **OSTα** and **OSTβ** (decreased and increased circles), which likely will reduce its activity, dominated by the limiting levels of OSTα. (Grey circles denote genes without altered expression after AMO/CLA incubation and genes, which were not analysed – OATPs.)

All the genes in red are genes affected by AMO/CLA.

Explanatory notes: ABCG5/8 – ATP-binding cassette G5/8; AMO/CLA – Amoxicillin/clavulanic acid; BAs – Bile acids; BSEP – Bile salt export pump; CYP7A1 – Cytochrome P450 7A1; CYP8B1 – Cytochrome P450 8B1; FXR – Farnesoid X receptor; MDR3 – Multidrug resistance protein 3; MRP2/3/4 – Multidrug resistance-associated protein 2/3/4; NTCP – Na^+-taurocholate co-transporting polypeptide; OA^- – Organic anions; OATPs – Organic anion transporting polypeptides; OSTα – Organic solute transporter α; OSTβ – Organic solute transporter β; SHP – Small heterodimer partner.

8 CONCLUSION

The hepatotoxic effects of AMO and AMO/CLA were assessed using HepG2 and human Upcyte hepatocytes. First of all, non-cytotoxic concentrations of AMO and AMO/CLA were evaluated using the MTT cell viability tests, and then after treatment with the studied drugs for 24 hours, the mRNA levels of crucial BA transporters, enzymes and NRs were measured by q-RT-PCR. The human Upcyte hepatocytes, especially when cultured between two collagen type-I layers, were proven to be more suitable cellular model for hepatotoxicity assessment of AMO/CLA.

Whereas AMO triggered significant alterations in gene expression of only two canalicular transporters (induction of MRP2 and MDR3), the effect of AMO/CLA was more widespread and extensive. Several changes were seen in the Upcyte cells incubated with AMO/CLA which can be explained as either pro-cholestatic mechanisms or compensatory responses to get rid of excessive BAs. The inhibition of canalicular BSEP and ABCG5/8 could lead to a decreased secretion of BAs and cholesterol, respectively. On the grounds of increasing concentration of BAs and cholesterol within hepatocytes, an inhibition of BA uptake via basolateral NTCP and an enhanced BA efflux via canalicular MRP2 could play a role as adaptive mechanisms. Moreover, decreased gene expression seen in CYP7A1, -8B1 and -27A1 caused *de novo* BA synthesis to be lowered. The inhibition of CYP7A1 and CYP8B1 expression agreed with the increased levels of SHP.

The Upcyte cells incubated with AMO and AMO/CLA were also evaluated for the protein expression of NTCP and BSEP. The protein expression level of NTCP was lower after treatment with AMO/CLA which agreed with reduced mRNA expression level. Unfortunately, the BSEP protein was not detected under the used conditions. Besides that, the image documentation of both treated hepatocellular models, provided by using digital microscopy, showed cytopathic effects in agreement with the MTT tests.

In conclusion, the performed experiments and the obtained results demonstrate for the first time that AMO and AMO/CLA can alter the gene expression of key hepatobiliary transporters, enzymes and NRs. Among the different observed effects of AMO/CLA, the inhibition of canalicular BSEP expression, which is crucial for BA efflux into the bile, could represent the most significant pro-cholestatic effect discovered here, though deregulation of other BA-related genes could also play important roles.

9 REFERENCES

Abboud G and Kaplowitz N. Drug-Induced Liver Injury. *Drug Safety* 2007;30(4): 277–94.

Andrade RJ et al. Drug-Induced Liver Injury: An analysis of 461 incidences submitted to the Spanish Registry over a 10-year period. *Gastroenterology* 2005;129(2): 512–21.

Andrade RJ, Camargo R, Lucena IM, and González-Grande R. Causality assessment in Drug-Induced Hepatotoxicity. *Expert Opinion on Drug Safety* 2004;3(4):329–44.

Bakke OM, Manocchia M, De Abajo F, Kaitin KI and Lasagna L. Drug safety discontinuations in the United Kingdom, the United States, and Spain from 1974 through 1993: A regulatory perspective. *Clinical Pharmacology & Therapeutics* 1995;58(1):108–17.

Ballatori N et al. OSTa-OSTb: A major basolateral bile acid and steroid transporter in human intestinal, renal, and biliary epithelia. *Hepatology* 2005;42:1270–279.

Ballatori N, Li N, Fang F, Boyer JL, Christian WV and Hammond CL. Ost alpha-Ost beta: A key membrane transporter of bile acids and conjugated steroids. *Frontiers Bioscience* 2010;14:2829–44.

Barbier O et al. FXR induces the UGT2B4 enzyme in hepatocytes: A potential mechanism of negative feedback control of FXR activity. *Gastroenterology* 2003;124:1926–40.

Bénichou C. Criteria of Drug-Induced Liver Disorders. *Journal of Hepatology* 1990;11(2):272–76.

Bennett PN, Brown MJ and Sharma P. *Clinical Pharmacology*. 11th ed. Churchill Livingstone Elsevier, 2012.

Björnsson ES, Bergmann OM, Björnsson HK, Kvaran RB and Olafsson S. Incidence, presentation, and outcomes in patients with Drug-Induced Liver Injury in the general population of Iceland. *Gastroenterology* 2013;144(7):1419–25.

Boyer JL et al. Upregulation of a basolateral FXR-dependent bile ccid efflux transporter OSTα-OSTb in cholestasis in humans and rodents. *American Journal of Physiology – Gastrointestinal and Liver Physiology* 2006;290:1124–30.

Bradford MM. A rapid and sensitive method for the quantitation of microgram quantities of protein utilizing the principle of protein-dye binding.” *Analytical Biochemistry* 1976;72(1–2):248–54.

Brunton LL, Chabner AB and Knollmann BC, eds. *Goodman & Gilman’s Pharmacological Basis of Therapeutics*. 12th ed. The McGraw-Hill Copanies, 2011.

Byrne JA, Strautnieks SS, Mieli-Vergani G, Higgins CF, Linton KJ and Thompson RJ. The Human Bile Salt Export Pump: Characterization of substrate specifity and identification of inhibitors. *Gastroenterology* 2002;123:1649–58.

Chalasani N et al. Causes, clinical features, and outcomes from a prospective study of Drug-Induced Liver Injury in the United States. *Gastroenterology* 2008;135(6): 1924–34.

Chang R, Chou MC, Hung LY, Wang ME, Hsu MC and Chiu CH. Study of valproic acid-enhanced hepatocyte steatosis. *BioMed Research International* 2016; 2016:1–11.

Chen M, Borlak J and Tong W. High lipophilicity and high daily dose of oral medications are associated with significant risk for Drug-Induced Liver Injury. *Hepatology* 2013;58(1):388–96.

Chiang JYL. Bile acid regulation of gene expression: Roles of nuclear hormone receptors. *Endocrine Reviews* 2002;23(4):443–63.

Chiang JYL. Bile acids: Regulation of synthesis. *Journal of Lipid Research* 2009;50(10):1955–66.

Chiang JYL. Bile acid metabolism and signaling. *Comprehensive Physiology* 2013; 3:1191–1212.

Chiang JYL. Recent advances in understanding bile acid homeostasis. *F1000 Research* 2017;6:2029–37.

Clark MA, Finkel R, Rey JA and Whalen K. *Lippincott's Illustrated Reviews: Pharmacology*. 5th ed. Lippincott Williams & Wilkins, 2012.

Danan G and Bénichou C. Causality assessment of adverse reactions to drugs - A novel method based on the conclusions of international consensus meetings: Application to Drug-Induced Liver Injuries. *Journal of Clinical Epidemiology* 1993;46(11):1323–30.

Dawson PA, Lan T and Rao A. Bile Acid Transporters. *The Journal of Lipid Research* 2009;50:2340–57.

De Abrew KN et al. Grouping 34 chemicals based on mode of action using connectivity mapping. *Toxicological Sciences* 2016;151(2):447–61.

Degen HJ, Deufel A, Eisel D, Grünewald-Janho S and Keesey J. *PCR Applications Manual*. 3rd ed. Roche Applied Sciences, 2006.

deLemos AS et al. Amoxicillin-Clavulanate-Induced Liver Injury. *Digestive Diseases and Sciences* 2016;61(8):2406–16.

Denson LA et al. The orphan nuclear receptor, SHP, mediates bile acid-induced inhibition of the rat bile acid transporter, NTCP. *Gastroenterology* 2001;121(1):140–47.

Donaldson PT et al. Human Leucocyte Antigen class II genotype in susceptibility and resistance to Co-Amoxiclav-Induced Liver Injury. *Journal of Hepatology* 2010;53(6):1049–53.

Donato MT, Jover R and Gómez-Lechón MJ. Hepatic cell lines for drug hepatotoxicity testing: Limitations and strategies to upgrade their metabolic competence by gene engineering. *Current Drug Metabolism* 2013;14:946–68.

Donato MT, López-Riera M, Castell JV, Gómez-Lechón MJ and Jover R. Both cholestatic and steatotic drugs trigger extensive alterations in the mRNA level of biliary transporters in rat hepatocytes: Application to develop new predictive biomarkers for early drug development. *Toxicology Letters* 2016;263:58–67.

Fernández-Murga ML, Petrov PD, Conde I, Castell JV, Goméz-Lechón MJ and Jover R. Advances in Drug-Induced Cholestasis: Clinical perspectives, potential mechanisms and *in vitro* systems. *Food and Chemical Toxicology* 2018; 120:196–212.

Fontana RJ. et al. Standardization of nomenclature and causality assessment in Drug-Induced Liver Injury: Summary of a clinical research workshop. *Hepatology* 2010;52(2):730–42.

Garzel B, Yang H, Zhang L, Huang SM, Polli JE and Wang H. The role of Bile Salt Export Pump gene repression in Drug-Induced Cholestatic Liver Toxicity. *Drug Metabolism and Disposition* 2004;42:318–22.

Graf GA et al. ABCG5 and ABCG8 are obligate heterodimers for protein trafficking and biliary cholesterol excretion. *The Journal of Biological Chemistry* 2003;278(48):48275–82.

Goodwin B et al. A regulatory cascade of the nuclear receptors FXR, SHP1, and LRH1 represses bile acid biosynthesis. *Molecular Cell* 2000;6:517–26.

Hagenbuch B and Dawson P. The Sodium Bile Salt Cotransport family SLC10. *European Journal of Physiology* 2004;(447):566–70.

Hagenbuch B and Meier PJ. Molecular cloning, chromosomal localization, and functional characterization of a human liver Na^+/bile acid cotransporter. *The American Society for Clinical Investigation* 1994;93:1326–31.

Hillman L et al. Clinical features and outcomes of complementary and alternative medicine induced Acute Liver Failure and Injury. *The American Journal of Gastroenterology* 2016;111(7):958–65.

Hollinger MA. *Introduction to Pharmacology*. 2nd ed. Taylor & Francis, 2003.

Hussaini HS and Farrington EA. Idiosyncratic Drug-Induced Liver Injury: An overview. *Expert Opinion on Drug Safety* 2007;6(6):673–84.

Konig J, Nies AT, Cui Y, Leier I and Keppler D. Conjugate export pumps of the Multidrug Resistance Protein (MRP) family: Localization, substrate specificity, and MRP2-mediated drug resistance. *Biochimica et Biophysica Acta* 1999; 1461:377–94.

Kool M et al. MRP3, an organic anion transporter able to transport anti-cancer drugs. *Proceedings of the National Academy of Sciences of the USA* 1999;96:6914–19.

Lammert C, Einarsson S, Saha C, Niklasson A, Björnsson E and Chalasani N. Relationship between daily dose of oral medications and idiosyncratic Drug-Induced Liver Injury: Search for signals. *Hepatology* 2008;47(6):2003–9.

Le Vee M, Lecureur V, Stieger B and Fardel O. Regulation of drug transporter expression in human hepatocytes exposed to the proinflammatory cytokines Tumor Necrosis Factor-Alfa or Interleukin-6. *Drug Metabolism and Disposition* 2009;37:685–93.

Lee J et al. Exploration of biomarkers for Amoxicillin/Clavulanate-Induced Liver Injury: Multi-omics approaches. *Clinical and Translation Science* 2017; 10(3): 163–71.

Lee WM. Drug-Induced Acute Liver Failure. *Clinics in Liver Diseases* 2013; 17(4):1–15.

Lehmann MJ et al. Activation of the nuclear receptor LXR by oxysterols defines a new hormone response pathway. *The Journal of Biological Chemistry* 1997;272(6):3137–41.

Leise MD, Poterucha JJ Talwalkar JA. Drug-Induced Liver Injury. *Mayo Clinic Proceedings* 2014;89(1):95–106.

Levy G et al. Long-term culture and expansion of primary human hepatocytes. *Nature biotechnology* 2015: 1–10.

López-Riera M et al. New microRNA biomarkers for Drug-Induced Steatosis and their potential to predict the contribution of drugs to Non-Alcoholic Fatty Liver Disease. *Frontiers in Pharmacology* 2017;8:1–12.

Lucena MI et al. Determinants of the clinical expression of Amoxicillin-Clavulanate Hepatotoxicity: A prospective series from Spain. *Hepatology* 2006;44(4):850–56.

Lucena MI et al. Phenotypic characterization of Idiosyncratic Drug-Induced Liver Injury: The influence of age and sex. *Hepatology* 2009;49(6):2001–9.

Lüllmann H, Mohr K and Wehling M. *Farmakologie a Toxikologie*. Grada Publishing, spol. s.r.o., 2002.

Mahmood T and Yang PC. Western Blot: Technique, theory, and trouble shooting. North American Journal of Medical Sciences 2012;4(9):429–34.

Meier Yvonne et al. Incidence of Drug-Induced Liver Injury in medical inpatients. *European Journal of Clinical Pharmacology* 2005;61(2):135–43.

Mikkaichi T, Suzuki T, Tanemoto M, Ito S and Abe T. The Organic Anion Transporter (OATP) family. *Drug Metabolism and Pharmacokinetics* 2004;19(3):171–79.

Mohi-ud-din R and Lewis JH. Drug- and Chemical-Induced Cholestasis. *Clinics in Liver Diseases* 2004;8(1):95–132.

Morgan RE et al. Interference with Bile Salt Export Pump function is a susceptibility factor for Human Liver Injury in drug development. *Toxicological Sciences* 2010;118(2):485–500.

Morita SY and Terada T. Molecular mechanisms for biliary phospholipid and drug efflux mediated by ABCB4 and bile salts. *BioMed Research International* 2014;2014:1–11.

Mosmann T. Rapid colorimetric assay for cellular growth and survival: Application to proliferation and cytotoxicity assays. *Journal of Immunological Methods* 1983;65(1–2):55–63.

Palmeira CM and Rolo AP. Mitochondrially-mediated toxicity of bile acids. *Toxicology* 2004;203(1–3):1–15.

Pauli-Magnus C and Meier PJ. Hepatobiliary transporters and Drug-Induced Cholestasis. *Hepatology* 2006;44:778–87.

Petrov PD, Fernández-Murga ML, López-Riera M, Goméz-Lechón MJ, Castell JV and Jover R. Predicting drug-induced cholestasis: Preclinical models. *Expert Opinion on Drug Metabolism & Toxicology* 2018;14(7):721–38.

Pontén F, Jirstrom K. and Uhlen M. The Human Protein Atlas - a tool for pathology. *The Journal of Pathology* 2008;216(4):387–93.

Rifkind D and Freeman GL. *The Nobel Prize Winning Discoveries in Infectious Diseases*. Elsevier Academic Press, 2005:44–5.

Robles M, Toscano E, Cotta J, Lucena MI and Andrade RJ. Antibiotic-Induced Liver Toxicity: Mechanisms, clinical features and causality assessment. *Current drug safety* 2010;5(3):212–22.

Sgro C et al. Incidence of Drug-Induced Hepatic Injuries: A French population-based study. *Hepatology* 2002;36(2):451–55.

Schaap FG, Trauner M and Jansen PLM. Bile Acid Receptors as Targets for Drug Development. *Nature Reviews Gastroenterology & Hepatology* 2013;11(1):55–67.

Silva MFB et al. Synthesis and intramitochondrial levels of valproyl-coenzyme A metabolites. *Analytical Biochemistry* 2001;290(1):60–67.

Singh D, Cho WC and Upadhyay G. Drug-Induced Liver Toxicity and prevention by herbal antioxidants: An overview. *Frontiers in Physiology* 2016;6:1–18.

Sittampalam GS, Coussens NP and Brimacombe K. Assay Guidance Manual. *Eli Lily Company and the National Center for Advancing Translational Sciences*, 2004.

Starkey Lewis PJ et al. Circulating microRNAs as potential markers of human Drug-Induced Liver Injury. *Hepatology* 2011;54(5):1767–76.

Stieger B, Fattinger K, Madon J, Kullak-Ublick GA and Meier PJ. Drug- and Estrogen-Induced Cholestasis through inhibition of the hepatocellular Bile Salt Export Pump (BSEP) of rat liver. *Gastroenterology* 2000;118:422–30.

Sundaram V and Björnsson ES. Drug-Induced Cholestasis. *Hepatology Communications* 2017;1(8):726–35.

Tolosa L et al. Human Upcyte Hepatocytes: Characterization of the hepatic phenotype and evaluation for acute and long-term hepatotoxicity routine testing. *Toxicological Sciences* 2016;152(1):214–29.

Tolosa L, Jiménez N, Pérez G, Castell JV, Gómez-Lechón MJ and Donato MT. Customised *in vitro* model to detect human metabolism-dependent idiosyncratic Drug-Induced Liver Injury. *Archives of Toxicology* 2018.

Wagner M, Zollner G and Trauner M. New molecular insights into the mechanisms of cholestasis. *Journal of Hepatology* 2009;51(3):565–80.

Wang K et al. Circulating microRNAs, potential biomarkers for Drug-Induced Liver Injury. *Proceedings of the National Academy of Sciences of the USA* 2009; 106(11):4402–7.

Watkins PB and Seeff LB. Drug-Induced Liver Injury: Summary of a single topic clinical research conference. *Hepatology* 2006;43(3): 618–31.

Wilkening S, Stahl F and Bader A. Comparison of primary human hepatocytes and hepatoma cell line HepG2 with regard to their biotransformation properties. *Drug Metabolism and Disposition* 2003;31(8):1035–42.

Williams KM, Arthur SJ, Burrell G, Kelly F, Phillips DW and Marshall T. An evaluation of protein assays for quantitative determination of drugs. *Journal of Biochemical and Biophysical Methods* 2003;57(1):45–55.

Zimmerman HJ and Ishak KG. Valproate-Induced Hepatic Injury: Analyses of 23 fatal cases. *Hepatology* 1982;2(5):591–97.

Zollner G et al. Hepatobiliary transporter expression in percutaneous liver biopsies of patients with Cholestatic Liver Diseases. *Hepatology* 2001;43.

Compound summary for Amoxicillin. In: *PubChem – Open chemistry database*. 2017a. Available at: https://pubchem.ncbi.nlm.nih.gov/compound/33613#section=Top. Access 1.10.2017

Compound summary for Clavulanic acid. In: *PubChem – Open chemistry database*. 2017b. Available at: https://pubchem.ncbi.nlm.nih.gov/compound/5280980#section=Top. Access 1.10.2017

Compound summary for Valproic acid. In: *PubChem – Open chemistry database*. 2017c. Available at: https://pubchem.ncbi.nlm.nih.gov/compound/3121#section=Top. Access 1.10.2017

Summary of product characteristics Amoksiklav 625 mg tbl flm 21. In: *SÚKL – Státní ústav pro kontrolu léčiv*. 2017. Available at: http://www.sukl.cz/modules/medication/detail.php?code=0085525&tab=texts. Access 9.10.2017